

1  
2  
3  
4  
5  
6  
7  
8  
9  
10  
11  
12  
13  
14  
15  
16  
17  
18  
19  
20  
21  
22  
23  
24  
25  
26  
27  
28  
29  
30

Humic surface waters of frozen peat bogs (permafrost zone)  
are highly resistant to bio- and photodegradation

Liudmila S. Shirokova<sup>1,2</sup>, Artem V. Chupakov<sup>2</sup>, Svetlana A. Zabelina<sup>2</sup>,  
Natalia V. Neverova<sup>2</sup>, Dahedrey Payandi-Rolland<sup>1</sup>, Carole Causserand<sup>1</sup>,  
Jan Karlsson<sup>3</sup>, Oleg S. Pokrovsky<sup>1,4\*</sup>

<sup>1</sup> Geoscience and Environment Toulouse, UMR 5563 CNRS, University of Toulouse, 14 Avenue  
Edouard Belin, Toulouse 31400, France

<sup>2</sup> Institute of Ecological Problems of the North, N. Laverov Federal Center for Integrated Arctic  
Research, Nab Severnoi Dviny 23, Arkhangelsk 163000, Russia

<sup>3</sup> Climate Impacts Research Centre (CIRC), Department of Ecology and Environmental Science,  
Umeå University, 901 87 Umeå, Sweden

<sup>4</sup> BIO-GEO-CLIM Laboratory, Tomsk State University, 35 Lenina Pr., Tomsk 634050, Russia

\*corresponding author email: [oleg.pokrovsky@get.omp.eu](mailto:oleg.pokrovsky@get.omp.eu)

Key words: depression, stream, river, organic carbon, photolysis, respiration, palsa, permafrost

Submitted to *Biogeosciences*, after revision May 2019

31 **Abstract**

32 Bio- and photo-degradation of dissolved organic matter (DOM) is identified as dominant vector  
33 of C cycle in boreal and high-latitude surface waters. In contrast to large number of studies of  
34 humic waters from permafrost-free regions and oligotrophic waters from permafrost-bearing  
35 regions, the bio- and photo-lability of DOM from humic surface waters of permafrost-bearing  
36 regions has not been thoroughly evaluated. Following standardized protocol, we measured  
37 biodegradation (low, intermediate, high temperature) and photodegradation (one intermediate  
38 temperature) of DOM in surface waters along the hydrological continuum (depression → stream  
39 → thermokarst lake → river Pechora) within a European Russian frozen peatland. In all systems,  
40 within the experimental resolution of 5 to 10%, there was no bio- or photodegradation of DOM  
41 over 1 month of incubation. It is possible that the main cause of the lack of degradation is the  
42 dominance of allochthonous refractory (soil, peat) DOM in all studied waters. Yet, all surface  
43 waters were supersaturated with CO<sub>2</sub>. Thus, this study suggests that, rather than bio- and photo-  
44 degradation of DOM in the water column, other factors such as peat porewater DOM processing  
45 and respiration of sediments are the main drivers of elevated pCO<sub>2</sub> and emission in humic boreal  
46 waters of frozen peat bogs.

47

48 **Introduction**

49 Boreal and subarctic waters contain large amounts of plant, soil, and peat-originated  
50 dissolved organic matter (Wilkinson et al., 2013; Kaiser et al., 2017), and the proportion of land-  
51 derived organic carbon in waters is likely to increase with ongoing permafrost thaw (Wauthy et  
52 al., 2018). Heterotrophic bacteria degrade this DOM (Karlsson, 2007; McCallister and del  
53 Georgio, 2008), causing net heterotrophic conditions (Gross Primary Productivity < Respiration)  
54 and CO<sub>2</sub> emission to the atmosphere from surface waters (Ask et al., 2012; Lapierre et al., 2013).  
55 Between 10% and 40% of the dissolved organic carbon (DOC) in lakes, rivers and soil waters

56 of the boreal zone may be available for bacterial uptake over a time frame of several weeks  
57 (Berggren et al., 2010; Roehm et al., 2009). The biodegradability of DOM leached from  
58 permafrost and non-permafrost soils was recently reviewed by Vonk et al. (2015) who concluded  
59 that aquatic DOC is more biodegradable in regions with continuous permafrost compared to  
60 regions without permafrost. At the same time, among all Arctic rivers, the highest annual (20%)  
61 and winter (ca. 45%) biodegradable DOC (BDOC) was reported for the Ob River, draining  
62 through peatlands with minimal influence of permafrost (Wickland et al., 2012). Further, based  
63 on 14 studies of BDOC and their own research, Vonk et al. (2015) demonstrated zero BDOC loss  
64 in aquatic systems without permafrost, which is contradictory to general understanding of  
65 biodegradation of aquatic DOM as major driver of CO<sub>2</sub> emission in boreal waters. It is also  
66 important to note that all the available bio-degradation studies of inland waters in permafrost  
67 regions dealt with either tundra ecosystems with shallow peat soils overlaying the mineral  
68 substrate or mountain regions with essentially mineral soil substrates in Alaska or Canada  
69 (Holmes et al., 2008; Wickland et al., 2012; Ward et al., 2017) and with the yedoma soils of  
70 Eastern Siberia (Mann et al., 2014, 2015; Spencer et al., 2015).

71 Similarly, although the photolysis of DOM in boreal and subarctic aquatic environments  
72 contributes to CO<sub>2</sub> emission from the inland waters to the atmosphere (Cory et al., 2014), the  
73 overwhelming majority of photo-degradation studies in the Arctic were conducted on oligotrophic  
74 lake waters and streams draining mineral soils of mountain regions (Ward and Cory, 2016; Cory  
75 et al., 2013, 2015). The dominance of photolytic processes in DOM processing in arctic waters  
76 was reported for N America (Cory et al., 2014; Ward et al., 2017), Canadian surface waters of  
77 the temperate zone (Winter et al., 2007; Porcal et al., 2013, 2014, 2015), and small Swedish  
78 humic-rich headwater catchments (Köhler et al., 2002). In contrast, several other studies from  
79 Scandinavia (Groeneveld et al., 2016; Koehler et al., 2014), Canada (Laurion and Mladenov,  
80 2013; Gareis and Lesack, 2018) and NW Russia (Oleinikova et al., 2017; Chupakova et al., 2018)

81 demonstrated sizeable removal of colored (chromophoric DOM) but quite small ( $\leq 10\%$ ) impact  
82 of sunlight irradiation on bulk DOC concentration in streams, rivers and lakes. Note here that the  
83 interaction between photo- and bio-degradation is more important than the individual processes  
84 as photo-oxidation may transform DOM molecular structures into more bioavailable forms (e.g.,  
85 Cory and Kling, 2018; Sulzberger et al., 2019).

86 Overall, available data demonstrate that an emerging paradigm on the importance of bio-  
87 and photodegradation may not be as consistent across the Arctic as previously thought, which  
88 call a need for further studies of these processes, encompassing wider range of aquatic settings.  
89 The numerous surface waters located within discontinuous to continuous permafrost zone of  
90 Northern Eurasia, where most aquatic systems are drained through frozen peat rather than mineral  
91 substrates, are poorly studied regarding bio- and photo-degradability of aquatic DOM. Yet, these  
92 regions (NE European Russia or Bolshezemelskaya tundra, Western Siberia Lowland, Northern  
93 Siberian Lowland, Kolyma and Yana-Indigirka Lowland) occupy  $> 2$  million km<sup>2</sup> which is more  
94 than 10% of overall permafrost-affected land area and exhibit, in average, ten times higher  
95 concentration of soil organic C in the form of 0.5 to 3 m thick peat layer than the rest of the  
96 circumpolar regions (Tarnocai et al., 2009; Raudina et al., 2018). As a result of the dominance  
97 of histosols, the surface waters draining frozen peatlands are enriched in DOC compared to other  
98 permafrost-affected regions (Manasypov et al., 2014; Pokrovsky et al., 2015) and may provide  
99 disproportionally high contribution to overall DOM bio- and photo-degradability in the Arctic  
100 and subarctic regions.

101 Numerous experiments in permafrost-bearing and permafrost-free aquatic environments  
102 including both organic and mineral soil substrates relatively poor in DOC demonstrated that the  
103 headwater streams and soil leachate contain most bio-degradable and photo-degradable DOM  
104 (Ilina et al., 2014; Mann et al., 2014, 2015; Larouche et al., 2015; Spencer et al., 2015; Vonk et  
105 al., 2015). Photo-oxidation and biodegradation were also shown to play **an** important role in small

106 streams of temperate peatlands of UK and Scotland (Moody et al., 2013; Pickard et al., 2017;  
107 Dean et al., 2019). In the present study, we hypothesized that, given nutrient-poor nature of  
108 Sphagnum peat from histosols, the bioavailability of essentially recalcitrant DOM in surface  
109 waters of frozen peatlands will be low. However, we expected a gradient in the degree of bio-  
110 and photo-lability of DOM from permafrost subsidence, head water stream, thermokarst lake and  
111 large river, corresponding to the increase in water residence time (Mann et al., 2012).

112 To test these hypotheses, we used recommended standardized protocol for DOM  
113 biodegradation (Vonk et al., 2015) and applied it for 4 main aquatic components of a hydrological  
114 continuum ‘permafrost subsidence → small stream → large thermokarst lake → large river  
115 (Pechora)’. We chose the largest frozen peatlands in Europe, the Bolshezemelskaya Tundra of  
116 NE European Russia which is represented by flat-mound (palsa) peat bog (discontinuous and  
117 continuous permafrost zone) and belongs to the watershed of the largest European permafrost-  
118 affected river, Pechora. Specific questions of this study were (i) to assess the difference in BDOC  
119 and photodegradable (PDOC) fraction of DOM in surface waters of frozen peat bog along the  
120 hydrological continuum, from permafrost depression to large rivers, (ii) to quantify the impact  
121 of temperature on biodegradation potential of surface waters from frozen peatbogs and predict  
122 possible impact of warming on DOM biodegradation efficiency, and (iii) to relate the BDOC and  
123 PDOC concentrations to the snapshot CO<sub>2</sub> concentration and emission.

124

125

## 126 **2. Study site and methods**

### 127 *2.1. Geographical context and hydrological continuum of the Pechora River basin*

128 The water samples were collected in the middle of July 2017 which is the middle summer  
129 period, consistent with time used by other researchers for biodegradation assays. The  
130 BolsheZemelskaya Tundra (BZT) peatland (continuous to discontinuous permafrost zone)

131 belongs to the Pechora River watershed (**Fig. S1**), the largest European Arctic river draining  
132 permafrost-bearing terrain (watershed = 322,000 km<sup>2</sup>; mean annual discharge is 4140 m<sup>3</sup>/s). The  
133 northern part of the Pechora watershed is covered by permafrost: discontinuous on the eastern  
134 part and sporadic to isolated on the western part (Brittain et al., 2009). The BZT is a hilly moraine  
135 lowland located between rivers Pechora and Usa (from the west and south) and the Polar Ural  
136 and Pai-Khoi ridge from the east. The dominant altitudes are between 100 and 150 m, created by  
137 hills and moraine ridges, composed of sands and silt with boulders. Between the moraines and  
138 ridges there are many lakes, mostly of thermokarst origin. The dominant soils are histosols of  
139 peat bogs and podzol-gleys in the southern forest-tundra zone. The mean annual temperature is -  
140 3.1°C and the mean annual precipitation is 503 mm. The dominant vegetation of the tundra zone  
141 is mosses, lichens and dwarf shrubs. Over past decades, the lakes of BZT exhibited sizeable  
142 increase in summer time temperature and pCO<sub>2</sub>, presumably due to enhanced bacterial respiration  
143 of allochthonous DOM from thawing permafrost (Drake et al., 2019).

144 We sampled surface waters along the typical hydrological continuum shown in Fig. S1  
145 and consisting of 1) depression in the moss and lichen cover of upland frozen peat bog, filled by  
146 water from thawing of ground ice (permafrost subsidence, 2.5 x 3 m size and 0.3 m depth); 2)  
147 small stream (~2 km length) originated from upland peat bog; 3) small thermokarst lake Isino  
148 (S<sub>area</sub> = 0.005 km<sup>2</sup>) located within the peat bog, and 4) the Pechora River mainstream. Similar  
149 principle of the hydrological continuum was considered in the Kolyma River biodegradation  
150 experiments (Mann et al., 2012). The list of sampled water objects together with their physical,  
151 chemical, microbiological characteristics and parameters of CO<sub>2</sub> system is presented in **Table 1**.  
152 The surface waters were collected from the shore (depression and stream) or the PVC boat (r.  
153 Pechora and Lake Isino). The water samples were placed into 2-L Milli-Q pre-cleaned PVC jars  
154 and kept refrigerated until arrival to the laboratory, within 2-3 h after collection.

155

156           2.2. *Experimental set-up*

157           2.2.1. Biodegradation

158           For biodegradation assays we followed the standardized protocol for assessing  
159 biodegradable DOC of Arctic waters (Vonk et al., 2015). To facilitate the implementation of  
160 recommended protocol, we used exactly the same filter towers, inline filter holders, and vacuum  
161 devices as depicted in Vonk et al. (2015). Initial samples were filtered through pre-combusted  
162 (4.5 h at 450°C) Whatman GF/F filters of nominal poresize 0.7 µm. All the manipulations were  
163 performed in laminar hood box (class A100) under sterile environment; the working space was  
164 sterilized by UV light before preparation. Triplicate 30 mL aliquots of 0.7 µm-filtered water were  
165 placed into pre-combusted (4.5 h at 450°C) dark borosilicate glass bottles of 40 mL volume  
166 wrapped in Al foil to prevent any photolysis, without nutrient amendment and stored at 23±1°C  
167 in the dark in thermostat. The bottles were closed with sterilized PVC caps. As recommended,  
168 the caps were left loose and the bottles were shaken manually once a day avoiding the liquid  
169 touching the cap. The incubated samples were re-filtered through pre-combusted 0.7 µm GF/F  
170 filters using sterilized dismountable Sartorius 25 mm filter holder and a cleaned sterile syringe  
171 after 0, 2, 7, 14 and 28 days of exposure. All handling and sampling of bottles was performed in  
172 the laminar hood box under sterilized workspace. Filtered samples were acidified with 30 µL of  
173 concentrated (8.1 M) double distilled HCl, tightly capped and stored in the refrigerator before  
174 DOC analyses. Non-acidified portion of filtrate was used for pH, Specific Conductivity, DIC and  
175 UV<sub>254 nm</sub> and optical spectra measurement. Control runs were 0.22 µm sterile-filtered water which  
176 was incubated in parallel to experiments and re-filtered through 0.7 µm GF/F filters at the day of  
177 sampling.

178           In addition to this ‘classic’ protocol, we used alternative procedure of biodegradation  
179 experiments to test maximally possible DOM removal by bacteria. For this, we replaced initial  
180 0.7 µm GF/F filtration by 3 µm filtration through sterilized Nylon Sartorius membranes, to

181 increase the amount of bacterial cells capable to degrade DOM during incubation. The reason for  
182 that is that conventional 0.7  $\mu\text{m}$  (GF/F) filtration might remove too many microbial cells (Dean  
183 et al., 2018). Besides, re-filtration through the same filter pore size (0.7  $\mu\text{m}$ ) recommended in  
184 classic protocol may not necessarily remove the newly formed microbial biomass as the cell size  
185 of bacteria grown during incubation may not exceed 0.7  $\mu\text{m}$ . In this regard, initial 3  $\mu\text{m}$ -filtration  
186 is equivalent of 100% inoculum used by Vonk et al. (2015) and can be considered as maximal  
187 enhancement of DOM biodegradation without addition of nutrients. Further, instead of 0.7  $\mu\text{m}$   
188 refiltration for sampling, we employed 0.22  $\mu\text{m}$  filter pore size for DOC samplings during  
189 incubation. This allowed to remove all particulate organic carbon formed via microbial  
190 metabolism, as well as some newly grown microbial cells and therefore should enhance the  
191 degree of biodegradation calculated as the difference between initial 3  $\mu\text{m}$ -filtration and 0.22  $\mu\text{m}$   
192 filtration at the date of sampling. The control runs were filtered through sterile 0.22  $\mu\text{m}$  filters  
193 and incubated parallel to the experiments, following the standard approach for control abiotic  
194 experiments in incubation experiments (Köhler et al., 2002). They were re-filtered through 0.22  
195  $\mu\text{m}$  membrane at the day of experimental sampling. To insure the lack of DOC release from  
196 sterilized Nylon membrane, we run blank (Milli-Q) filtration through both 0.7  $\mu\text{m}$  GF/F and 0.22  
197  $\mu\text{m}$  Nylon filters; in both cases the DOC blank was below 0.1-0.2 mg/L which is less than 1% of  
198 DOC concentration in our samples. The glass bottles were incubated in triplicates at  $4\pm 2^\circ\text{C}$ ,  
199  $22\pm 1^\circ\text{C}$  and  $37\pm 3^\circ\text{C}$  using refrigerator and incubators and agitated manually at least once a day  
200 over 4 weeks of exposure.

201

### 202 2.2.2. Photodegradation

203 For photodegradation incubations, water samples of all sites except the river were  
204 collected in polypropylene jars and sterile filtered (0.22  $\mu\text{m}$  Nalgene Rapid-Flow Sterile  
205 Systems) within 2 h of sampling and refrigerated. The filtrates were transferred under laminar



206 hood box into sterilized, acid-washed quartz tubes (150 mL volume, 20% air headspace) and  
207 placed at  $3\pm 2$  cm depth into outdoor pool which was filled by river water having the light  
208 transparency similar to that of the Pechora River (1.5-2.0 m Secchi depth). In-situ measurements  
209 of sunlight intensity were conducted using submersible sunlight sensor. The outdoor pools were  
210 placed under unshaded area, at the latitude similar to that of the sampling sites. Slight wind  
211 movement and regular manual shaking allowed for sufficient mixing of the interior of reactors  
212 during exposure. All the experiments were run in triplicates. The water temperature was  $19\pm 3^{\circ}\text{C}$   
213 over 28 days of exposure (17 July - 14 August 2017), with an average magnitude of diurnal water  
214 temperature variation of  $6^{\circ}\text{C}$  (recorded every 3 h using EBRO EBI 20 Series loggers). The day  
215 light intensity was typically between 5,000 and 20,000 lux (in average 10,000 lux or  $14\pm 5 \text{ W/m}^2$ )  
216 which is within the range of solar radiation at the latitude of the polar circle during this period of  
217 the year. Overall, we followed conventional methodology for photodegradation which is  
218 exposure of  $0.2 \mu\text{m}$ -sterile filtered samples in quartz reactors in the outdoor pool (Vähätalo et al.,  
219 2003; Chupakova et al., 2018; Gareis and Lesack, 2018), solar simulator (Lou and Xie, 2006;  
220 Amado et al., 2014) or directly in the lake water (Laurion and Mladenov, 2013; Groeneveld et  
221 al., 2016). Note that the  $0.22 \mu\text{m}$  sterile filtration is the only way of conducting photodegradation  
222 experiments, given that the autoclave sterilization of DOM-rich natural water would coagulate  
223 humic material and thus is not suitable (Andresson et al., 2018). We have chosen 4 week  
224 exposure time for consistency with biodegradation experiments described above and following  
225 the previous studies on photodegradation under sunlight, which is typically from 15 to 70 days  
226 (Moran et al., 2000; Vähätalo and Wetzel, 2004; Mostofa et al., 2007; Helms et al., 2008;  
227 Chupakova et al., 2018). Dark control experiments were conducted in duplicates, using sterilized  
228 glass tubes filled by sterile  $0.22 \mu\text{m}$ -filtered water, wrapped in Al foil and placed in the same  
229 outdoor pool as the experiments. The headspace (approx. 20% of total reaction volume) was  
230 similar in experimental and control reactors. The individual reactors were sterile sampled at the

231 beginning and at the 2<sup>nd</sup>, 7<sup>th</sup>, 14<sup>th</sup>, 21<sup>th</sup> and 28<sup>th</sup> day of exposure. Each sampling sacrificed the  
232 entire reactor. The MilliQ blanks were collected and processed to monitor for any potential  
233 sample contamination introduced by our filtration, incubation, handling and sampling  
234 procedures. The organic carbon blanks of filtrates never exceeded 0.2 mg/L.

235

### 236 2.3. Analyses and treatment

237 The temperature, pH, O<sub>2</sub> and specific conductivity in surface waters were measured in  
238 the field as described previously (Shirokova et al., 2013b). Dissolved CO<sub>2</sub> concentration was  
239 measured using submersible Vaissala Carbocap® GM70 Hand-held carbon dioxide meter with  
240 GMP222 probes (accuracy 1.5%; see Serikova et al. (2018, 2019) for methodological details).  
241 The diffusional CO<sub>2</sub> flux was calculated using wind-based model (Cole and Caraco, 1998) with  
242  $k_{600} = 2.07 + 0.215 \times u_{10}^{1.7}$ , where  $u_{10}$  is the wind speed at 10 m height. In the filtrates, we measured  
243 optical density at 254 nm and at selected wavelengths (365, 436, 465, and 665 nm) of the visible  
244 spectrum. The specific UV-absorbency (SUVA<sub>254</sub>, L mg<sup>-1</sup> m<sup>-1</sup>) and E4:E6 ratios are used as a  
245 proxy for aromatic C, molecular weight and source of DOM (Weishaar et al., 2003; Peacock et  
246 al., 2013; Ilina et al., 2014).

247 The DOC and DIC were analyzed by high-temperature catalytic oxidation using TOC-  
248 VCSN, Shimadzu® (uncertainty ± 2%, 0.1 mg L<sup>-1</sup> detection limit). The DIC was measured after  
249 sample acidification with HCl and DOC was analyzed in acidified samples after sparging it with  
250 C-free air for 3 min at 100 mL min<sup>-1</sup> as non-purgable organic carbon (NPOC). Selected quartz  
251 reactors in photodegradation experiments were used to measure dissolved O<sub>2</sub> using Oxi 197i  
252 oximeter with a Cellox® 325 galvanic submersible sensor (WTW, Germany; ± 0.5%  
253 uncertainty). For this, the O<sub>2</sub> galvanic sensor was introduced into the quartz tube immediately  
254 after opening of the reactor and allowed to equilibrate for 5-10 min while protecting the open  
255 end of the tube from the exchange with atmospheric oxygen via wrapping it in Al foil. All filtered

256 sampled collected from photo-degradation experiments were acidified with ultrapure nitric acid  
 257 and analyzed for major and trace elements following procedures employed in GET (Toulouse)  
 258 for analyses of boreal humic waters (Oleinikova et al., 2017, 2018).

259 To account for possible microbial development in biodegradation experiments, we  
 260 performed oligotrophic and eutrophic bacteria count in the course of incubation, following the  
 261 standard methodology used in biodegradation experiments of peat waters (Stutter et al., 2013) as  
 262 also described previously (Shirokova et al., 2017b; Chupakova et al., 2018). In addition, we  
 263 measured total bacterial number and quantified the dominant cell size morphology using DAPI  
 264 fluorescence method (Porter and Feig, 1980). Control experiments did not demonstrate the  
 265 presence of any countable cells in the observation fields.

266 The bio- and photodegradable DOC (BDOC and PDOC, respectively) were calculated in  
 267 percent loss relative to control at each sampling time point  $t$  (0, 2, 7, 14 and 28 days) according  
 268 to:

$$269 \quad \text{BDOC}(\%)_t = 100\% \times (\text{DOC}_{t, \text{control}} - \text{DOC}_t) / \text{DOC}_{t, \text{control}} \quad (1)$$

270 Alternatively, the BDOC and PDOC were calculated in percent loss at time point  $t$  relative to the  
 271 initial concentration of DOC ( $\text{DOC}_{t=0}$ ) following Vonk et al. (2015):

$$272 \quad \text{BDOC}(\%)_t = 100\% \times (\text{DOC}_{t=0} - \text{DOC}_t) / \text{DOC}_{t=0} \quad (2)$$

273 For most treatments and sampled waters, the difference between two methods of bio-  
 274 /photodegradable DOC concentration was statistically negligible. To assess the variability of  
 275 results, shown as vertical uncertainties in the graphs, we used the percentage ratio of standard  
 276 deviation of  $n$  replicates at the  $i$ -th day of exposure to the initial DOC concentration following:

$$277 \quad SD_i = \sqrt{\frac{(\text{BDOC}_i^1 - \text{BDOC}_i^{\text{mean}})^2 + (\text{BDOC}_i^2 - \text{BDOC}_i^{\text{mean}})^2 + \dots + (\text{BDOC}_i^n - \text{BDOC}_i^{\text{mean}})^2}{n}} \quad (3)$$

$$278 \quad \%SD_i = \frac{SD_i}{\text{DOC}_0} \cdot 100 \quad (4)$$

279 The results are presented as % BOD<sub>*i*</sub> ±  $SD_i$ .

280 To assess the uncertainties during photodegradation experiments, we used the percentage of  
 281 standard deviation on  $n$  replicates at the  $i$ -th day of exposure to the DOC concentration in the  
 282 dark (control) reactors as

$$283 \quad PDOC_i^n = DOC_i^{blank} - DOC_i^n \quad (5)$$

$$284 \quad PDOC_i^{mean} = \frac{PDOC_i^1 + PDOC_i^2 + \dots + PDOC_i^n}{n} \quad (6)$$

$$285 \quad \%PDOC_i = \frac{PDOC_i^{mean}}{DOC_i^{blank}} \cdot 100 \quad (7)$$

$$286 \quad SD_i = \sqrt{\frac{(PDOC_i^1 - PDOC_i^{mean})^2 + (PDOC_i^2 - PDOC_i^{mean})^2 + \dots + (PDOC_i^n - PDOC_i^{mean})^2}{n}} \quad (8)$$

$$287 \quad \%SD_i = \frac{SD_i}{DOC_i^{blank}} \cdot 100 \quad (9)$$

288 The results are presented as  $\% PDOC_i \pm SD_i$

289 Note that in case of negative values provided by Eqn. 2, the BDOC was taken as 0% following  
 290 the conventional practice in biodegradation experiments (Vonk et al., 2015). The uncertainties  
 291 of BDOC % numbers were between  $\pm 5$  and  $\pm 10\%$  for experiments, at 4, 23 and 37°C using  
 292 modified (3  $\mu\text{m}$  and 0.22  $\mu\text{m}$  filtration) protocol. In ‘classic’ protocol (0.7  $\mu\text{m}$  GF/F filtration)  
 293 the uncertainties were as high as 10-15% at the end of experiment. We believe that such high  
 294 uncertainties are linked to high initial DOC concentration, triplicate measurements and  
 295 simultaneous monitoring of experimental and control runs.

296 Statistical treatment included the least squares method and the Pearson correlation,  
 297 because the data were normally distributed. The ANOVA method was used to test the differences  
 298 in the average DOC concentration versus time in incubation experiments and in the controls and  
 299 to assess the difference between the light experiments and the dark control for photo-degradation  
 300 experiments. All calculations were performed in STATISTICA ver. 10 (StatSoft Inc., Tulsa) at  $p$   
 301 = 0.05).

302

303

### 304 **3. Results**

#### 305 *3.1. Assessment of biodegradable DOC*

306 The waters of hydrological continuum within the Pechora River basin are highly diverse  
307 (**Table 1**), with pH range from 3.8 (frozen peat depression) to 6.9 (r. Pechora). The soluble salts  
308 concentrations are low as the specific conductivity ranged from  $20\pm 10 \mu\text{S cm}^{-1}$  (stream,  
309 thermokarst lake) to  $\sim 60 \mu\text{S cm}^{-1}$  in the peat bog depression and the Pechora River. The DOC  
310 concentration decreased from  $44 \text{ mg L}^{-1}$  in frozen peat depression to  $\sim 8 \text{ mg L}^{-1}$  in the Pechora  
311 River following the order of water residence time (flow direction) “depression  $\gg$  stream  $\geq$   
312 thermokarst lake  $>$  r. Pechora”. The DOC concentration was generally similar (within  $\pm 2\%$ )  
313 between 3, 0.7 and  $0.22 \mu\text{m}$  pore size filtration of the initial sample, in agreement with former  
314 size fractionation measurement in Arctic and subarctic systems (Vasyukova et al., 2010;  
315 Pokrovsky et al., 2012, 2016). All sampled surface waters exhibited  $\text{CO}_2$  supersaturation with  
316 respect to atmosphere (from 440 to 2400 ppm) and net  $\text{CO}_2$  emission (diffusion) flux ranging  
317 from 34 to  $74 \text{ mmol CO}_2 \text{ m}^{-2} \text{ d}^{-1}$  (**Table 1**).

318 In both protocols of biodegradation experiments, two major features were noted: (1) the  
319 concentrations of  $0.7 \mu\text{m}$  and  $0.22 \mu\text{m}$ -filtered DOC did not decrease during the exposure and  
320 (2) there was no sizable ( $> 10\%$ ) difference between the control run and the incubation  
321 experiment (**Fig. 1**). By ‘classic’ protocol of biodegradation experiments ( $0.7 \mu\text{m}$  GF/F filtration)  
322 at  $23^\circ\text{C}$ , the BDOC fraction ranged between 0 and 10 % for all surface waters. The modified  
323 procedure ( $3 \mu\text{m}$  initial filtration and  $0.22 \mu\text{m}$  sampling) did not detect any significant  
324 biodegradation for any of the studied waters (average equaled to  $5\pm 5\%$  at 4, 23 and  $37^\circ\text{C}$ , **Fig. 2**  
325 **B, C, D**). The DIC concentrations remained constant ( $\pm 5\%$  of the initial value) in all experiments,  
326 but increased in stream water incubated at  $37^\circ\text{C}$ , where we measured  $\sim 10\%$  increase over 28 days  
327 of exposure (not shown). This increase was equal to  $0.2 \text{ mg/L}$  of DIC. Note that equivalent  
328 decrease in DOC concentration could not be assessed, presumably due to instrument limitation

329 (the intrinsic uncertainty on NPOC analyses (ca. 2% of 15 mg/L of DOC) which did not allow  
330 measuring C change smaller than 0.3 mg/L.

331 The UV<sub>254 nm</sub> absorbency of samples in the course of dark aerobic exposure demonstrated  
332 slight decrease with time (ca., between 5 and 10% over 28 days) in peat bog depression by  
333 ‘classic’ protocol (**Fig. S2 of Supplement**). However, in all other treatments, the control was  
334 indistinguishable from experimental runs and the SUVA<sub>254</sub> remained constant within the  
335 uncertainties of triplicates (ca., ±5 to ±10%). Similarly, no measurable change in optical  
336 properties of DOM (absorbency at 365, 465, 665 nm and E4:E6 ratio) could be detected during  
337 exposition.

338 The microbial consortium of all systems was dominated by cocci (0.23 µm median size)  
339 and rods (0.96 x 0.20 µm) as revealed from DAPI fluorescent imaging. The number of culturable  
340 oligotrophic bacteria increased by a factor of ~ 100 after first 2-7 days of exposure at 22°C both  
341 in GF/F-filtered and 3µm-filtered samples, and then remained stable at ca. 10,000 to 20,000 CFU  
342 mL<sup>-1</sup> till the end of experiments (**Fig. S3 A, C**). The highest concentration of oligotrophic bacteria  
343 was observed in the Pechora River, where as the other samples were not significantly different  
344 between each other. The CFU value at 4°C ranged between 1000 and 5000 CFU mL<sup>-1</sup> and did  
345 not demonstrate any clear pattern with time of incubation (**Fig. S3 B**). The number of eutrophic  
346 bacteria ranged between 1,000 and 15,000 CFU mL<sup>-1</sup> following the order: r. Pechora > stream ≥  
347 peat bog depression ≥ thermokarst lake. There was no growth of eutrophic or oligotrophic  
348 bacteria at 37°C. The total cell number gradually increased in the course of experiment at 22°C  
349 (**Fig. S3 D**) with maximal changes observed in peatbog depression and the Pechora River (by a  
350 factor of 30 and 40, respectively). There was a progressive increase of rod-shaped bacillus  
351 relative to coccus in the Pechora River and a permafrost stream whereas the thermokarst lake and  
352 peatbog depression did no exhibit any systematic change in dominant bacteria morphologies  
353 during the biodegradation experiments. Note that the total cell number in surface waters of

354 Bolshezemelskaya Tundra were similar to those obtained in incubation experiments (see Table  
355 1, Fig. S3).

356

### 357 *3.2. Photodegradation of DOM from frozen peatlands*

358 The pH of sunlight-exposed samples did not exhibit any systematic variation within 0.5  
359 pH unit. The DIC remained fairly stable (within 0.5 mg/L) without any significant ( $R^2 < 0.5$ ;  $p >$   
360 0.05) change during incubation, regardless of the type of system, DOC and DIC concentration  
361 (not shown). The exposed water remained oxygenated (average O<sub>2</sub> saturation close to 90%) with  
362 no detectable change (i.e. > 10%) over the course of experiment. Specific conductivity also  
363 remained highly stable over full period of exposure.

364 The bacteria count in photo-degradation reactors at the beginning of exposure and after  
365 14 and 28 days of incubation yielded between 1 and 100 CFU mL<sup>-1</sup>. This is a factor of 100 to  
366 1000 lower than the number of cells in experiments of bio-degradation run in non-sterilized  
367 waters over the same duration of experiments (section 3.1). As such, the microbial degradation  
368 was considered negligible at our experimental conditions of sunlight exposure.

369 There was no sizeable decrease in DOC concentration during 28 d of exposure to sunlight  
370 (**Fig. 3 A**). This relative change of DOC concentration ranged from -5 % to +5 % and it did not  
371 exceed the non-systematic variability among triplicates. Although the triplicate agreed within  
372 less than 2 % (the symbol size in **Fig. 3**), the small change of DOC in peat depression was similar  
373 in light experiment and dark control. The % PDOC (relative to starting solution) as a function of  
374 exposure time over 28 days of experiment ranged from 0 to 5% in peatbog depression and 0 to  
375 10% in thermokarst lake and permafrost spring (**Fig 3 B**).

376 The SUVA<sub>254 nm</sub> in photodegradation experiments decreased much stronger than the  
377 DOC. The SUVA decrease relative to control was mostly pronounced in permafrost stream (**Fig.**  
378 **4**). The optical properties of DOC demonstrated sizeable decrease of E<sub>365</sub>/E<sub>470</sub> ratio

379 corresponding to UV/vis absorbing functional groups (**Fig. S4 A**), which was consistent with  
380 decreasing  $SUVA_{254\text{ nm}}$  during sunlight exposure. The  $E_{254}/E_{436}$  ratio, corresponding to  
381 autochthonous vs. terrestrial DOM, did not demonstrate any sizeable change over the course of  
382 experiment (**Fig. S4 B**).

383 Most of major and trace elements did not show any significant (at  $p < 0.05$ ) change in  
384 concentration over the photodegradation experiments. Only a few nutrients (P, Fe, Zn, B) and  
385 trace metals (Zn, Ti, V, Zr, Nb and Th) demonstrated a decrease in concentration. The decrease  
386 of Fe was mostly pronounced in permafrost stream, and did not occur in permafrost depression  
387 (**Fig. 5 A**) whereas total dissolved phosphorus systematically decreased, by 20 to 50%, over 28  
388 days of sunlight exposure in permafrost depression, thermokarst lake and permafrost stream (**Fig.**  
389 **5 B**). A decrease of Ti, Zn, Nb and Th also occurred in thermokarst lake and permafrost stream  
390 (not shown). Overall, the magnitude of decrease of P, Fe, Ti, V and Zn in photodegradation  
391 experiments followed the order “permafrost stream > thermokarst lake > permafrost depression”.

392

#### 393 **4. Discussion**

394 *4.1. High stability of dissolved organic matter to biodegradation in surface waters from*  
395 *frozen peatland*

396 The unexpected result of this study was very low BDOC fraction, measured not only in  
397 large river (Pechora) but also in small stream, thermokarst lake and peatland depressions formed  
398 due to permafrost subsidence. According to compilation of available biodegradation studies, the  
399 BDOC fraction (28 days of exposure) ranges from 3 to 18% (mean 13%) in waters of continuous  
400 permafrost zone and from 5 to 15% (mean 14%) in discontinuous permafrost zone (Vonk et al.,  
401 2015). This is higher than the 0 to 10 % of BDOC measured for all water objects from the  
402 discontinuous permafrost zone in this study. Note that very few biodegradability studies in  
403 aquatic systems dealt with frozen peatlands, and all previous incubation experiments used water



404 from mountainous regions on mineral soils in Scandinavia, Alaskan slope and Canada, yedoma  
405 regions of Eastern Siberia, or the Yenisey basin. Only one former biodegradation study in peat  
406 mire context demonstrated sizable bioavailability of soil leachate to lake water bacteria (Roehm  
407 et al., 2009), but this work did not deal with pure aquatic endmember, unlike this study. Instead,  
408 the BDOC of frozen peatlands surface waters measured for the Bolshezemelskaya Tundra inland  
409 waters was comparable with the value suggested by Vonk et al (2015) for non-permafrost aquatic  
410 DOC (0-1 %).

411 Another important point revealed in previous work on biodegradation of Arctic waters is  
412 that aquatic BDOC in large streams and rivers decreased as the Arctic summer progressed (Vonk  
413 et al., 2015), although this pattern was absent for soil leachates and small streams. In our case,  
414 thermokarst lake Isino and r. Pechora can be considered as sufficiently large hydrological  
415 systems. The sampling was performed in the end of July which is already summer baseflow  
416 period and as such 0 to 5 % biodegradable DOC measured for Isino and Pechora in this study is  
417 comparable with 0 to 20% BDOC loss reported in large streams and rivers at ~200 Julian day  
418 (Vonk et al., 2015). However, small stream and permafrost subsidence remain clearly at the very  
419 low edge of BDOC % lost reported for soils and streams in summer. In the estuarine zone of  
420 largest European Arctic permafrost-free river, Severnaya Dvina, there was no measurable  
421 biodegradation in spring, when the DOM was dominated by allochthonous sources, but a 15 to  
422 20% decrease of DOC occurred during first 300 h in river water collected in August, when  
423 sizeable phytoplankton productivity was observed (Shirokova et al., 2017b). In laboratory  
424 experiments with individual cultures, moss and peat leachates were also sizably biodegraded over  
425 1-2 days of exposure (Shirokova et al., 2017a), whereas the same bacterial species were not  
426 capable degrading DOM from surface waters draining peatland and moss covered bogs  
427 (Oleinikova et al., 2018). Following a recommended protocol of biodegradation assays (Vonk et  
428 al., 2015), in this work we incubated natural water without nutrients. This creates potential bias

429 for application of obtained results to various subarctic settings. For example, one should note that  
430 nutrients and labile DOM addition downstream (away from the oligotrophic bogs) can increase  
431 the capacity of bio-degradation and related CO<sub>2</sub> emission in large river, before its discharge to  
432 the Arctic Ocean. Further, it is possible that in natural settings, the input of biolabile DOC from  
433 terrestrial vegetation may enhance the bioavailability of stable DOC (e.g., Textor et al., 2018)  
434 although this effect could not be tested in this study.

435         Mechanistic reasons for extremely low bioavailability of DOC from studied peatlands  
436 remain unclear and require in-depth analysis of DOM molecular structure and stoichiometry as  
437 well as high resolution microbial approaches. It is known that the DOM released from frozen  
438 soils contains high proportions of biologically labile protein-like and photochemically reactive  
439 aromatic substances (Gao et al., 2018). Following the pioneering study of Ward et al. (2017),  
440 we hypothesize that, similar to DOC from organic (non-permafrost) layer, the concentration of  
441 high-lability, aliphatic-like DOC in surface waters of frozen peatlands is too low to sustain  
442 microbial population, or that this aquatic DOC, remaining after microbial processing of soil  
443 porewater DOC is of low lability for microbes capable to degrade aliphatic-like DOC and  
444 inhabiting aerobic zone of permafrost surface waters. The constant pattern of UV<sub>254</sub> absorbency  
445 in biodegradation experiment was consistent with negligible change in BDOC over 28 days of  
446 incubation. In comparison, the biodegradation of peat water from European boreal zone was  
447 associated with an increase in SUVA by up to 7.4 %, which also implies an increase in the  
448 proportion of aromatic compounds (Hulatt et al., 2014). The total bacterial number in studied  
449 surface waters  $(0.5-5) \times 10^6$  cell mL<sup>-1</sup> is in excellent agreement with other studies of thermokarst  
450 peatland lake waters (Deshpande et al., 2016). Following these researchers, we suggest that the  
451 reason of low biodegradability of peatland humic waters is that the majority of active bacteria  
452 are associated with particles (> 3 µm) rather than present as free-living cells (< 1 µm) capable to  
453 DOC processing. In addition, the bacterial communities are not just shaped by size fractionation

454 by filtration, but also the presence or absence of bacterial grazers (Dean et al., 2018). However,  
455 further mechanistic studies of model aquatic bacterial communities capable to affect the  
456 degradation of DOM from different terrestrial sources are necessary (Logue et al., 2016).

457 Interestingly, there was no measurable difference in BDOC at 4, 23 and 37°C, as the  
458 proportion of BDOC at all temperatures for each system was below 5-10%. This result allows  
459 preliminary prediction of possible consequence of climate change and surface water heating in  
460 high latitudes. In a short-term climate warmings scenario, or assuming fast heating of surface  
461 waters due to prolonged heat wave of draught occurring both in European, permafrost-free  
462 (Shirokova et al., 2013a) and western Siberian (Pokrovsky et al., 2013) permafrost-bearing  
463 peatlands, we do not foresee any measurable change in biodegradability of DOM from the water  
464 column. Under even most extreme heating scenario of thermokarst lakes, river and depressions  
465 of the frozen peatland territories, the short-term bio-processing of aquatic DOM may remain  
466 close to zero.

467

#### 468 *4.2. Negligible impact of photodegradation on DOM transformation in inland waters of* 469 *frozen peatlands*

470 The second main result of this work was high stability of surface waters DOM to sunlight  
471 exposure. Over 28 d of incubation in outdoor pools at the conditions corresponding to surface (<  
472 0.05 m depth) water layer of thermokarst lakes and streams from permafrost zone, the change in  
473 DOC concentration was less than 5-10% of the initial value and was not distinguishable from  
474 that in the dark control (**Fig. 3 A, B**). Therefore, the DOM of all frozen peatland is quite refractory  
475 and not subject to measurable photodegradation over 4 weeks of exposure. This period is  
476 comparable with the water residence time in small depressions of frozen peatlands (Novikov et  
477 al., 2009) and small thermokarst thaw ponds of frozen palsa peatbogs (Manasypov et al., 2015)  
478 but much higher than the water travel time in small streams (< 10 km long) and in the lower

479 reaches of Pechora river, from the site of sampling till the Arctic Ocean (ca. several days). This  
480 result apparently contradicts the recent paradigm that the photochemical oxidation may account  
481 for 70 to 95% of total DOC processed in the water column of arctic lakes, rivers and soils (Cory  
482 et al., 2013, 2014; Ward and Cory, 2016; Ward et al., 2017). However, the conclusion of this  
483 group of authors is based on study of distilled water leachates of mineral soils, headwater streams,  
484 fresh permafrost thaw sites and lakes of N. Alaska slopes, developed on mineral substrates. In  
485 contrast, the results of DOM photolysis in polygonal and runnel ponds located in frozen peatlands  
486 (2 m peat, 40-60 cm active layer thickness) of continuous permafrost regions (Canada High  
487 Arctic) demonstrated a relatively fast decay of **water** color and fluorescence, but insignificant  
488 losses of DOC over 12 days of exposure time (Laurion and Mladenov, 2013). Recently, no  
489 measurable photochemical loss of ancient permafrost DOC has been revealed in the thawing  
490 yedoma permafrost sites of the Kolyma River, its tributaries and streams (Stubbins et al., 2017).  
491 Another recent study of DOM photodegradation in boreal high-latitude peatland streams of the  
492 White Sea watershed demonstrated only 10% decrease in DOC concentration over 10 days of  
493 incubation under sunlight (Oleinikova et al., 2017). In the estuarine zone of the largest European  
494 Arctic river draining wetland- and forest-dominated permafrost-free territory (Severnaya Dvina),  
495 we did not find any measurable photo-degradation of DOM over 1 month of exposure  
496 (Chupakova et al., 2018). This comparison clearly demonstrates highly contrasting DOM  
497 photolability between the aquatic systems of N. America, draining through mineral soil  
498 substrates, and that of boreal and subarctic peatlands.

499 Further, due to high homogeneity of organic substrate surrounding studied waters and  
500 similar allochthonous origin of DOM in all surface waters of frozen peatlands, there was no  
501 dramatic difference in DOM photodegradability over the hydrological continuum in NE  
502 European Arctic, which also contrasts the results obtained in aquatic systems on mineral soils  
503 (Cory et al., 2007, 2013; Reader et al., 2014). It is possible that either 1) photochemical

504 degradation of humic peat waters occurs very fast, during first hours to days upon their exposure  
505 to sunlight or 2) that the nature of DOM is so refractory that much longer exposure periods, on  
506 the order of several months to years (as in the Arctic coast) are necessary to photodegrade the  
507 DOM from frozen peatlands. The first explanation is consistent with recent experiments on  
508 photodegradation of fresh peat mire water, collected in taiga region of NW Russia, where about  
509 50% of bogwater DOC was photodegraded over 2 days of exposure to sunlight (Oleinikova et  
510 al., 2017).

511 As such, it is possible that all surface waters sampled for experiments in this study,  
512 including stagnant water in permafrost depression, have already contacted with sunlight for more  
513 than several days and thus became photo-resistant. Assuming the maximal possible DOC loss  
514 due to photolysis assessed in our experiments ( $0.1 \text{ mg C L}^{-1} \text{ d}^{-1}$  corresponding to a loss of 3 mg/L  
515 during 28 days) and the light penetration depth of 0.5 m which is comparable with the typical  
516 depth of studied water bodies, the photodegradation can contribute to less than 10 % of total  $\text{CO}_2$   
517 emission flux from the water surfaces of frozen peatlands ( $0.4\text{-}0.8 \text{ g C m}^{-2} \text{ d}^{-1}$  in this work;  $0.8$   
518 to  $4.4 \text{ C m}^{-2} \text{ d}^{-1}$  in western Siberian rivers and streams, located on very similar context of frozen  
519 peat bogs, Serikova et al., 2018). The maximal PDOC value measured in this work is also at the  
520 lower end range of DOM photodegradation contribution to C flux in North European boreal and  
521 subarctic settings. Thus, DIC annual photo-production contributed between 1 and 8 % of  $\text{CO}_2$   
522 emissions from a humic lake in south of Sweden (Groeneveld et al., 2016) and globally in the  
523 boreal and subarctic zone, sunlight-induced  $\text{CO}_2$  emissions represent about one tenth to the  $\text{CO}_2$   
524 emission from lakes and reservoirs (Koehler et al., 2014).

525 The evolution of optical properties of DOM as a function of exposure time in different  
526 samples was consistent with the mechanisms of photo-sensitive DOM removal during irradiation.  
527 The ratio  $E_{365}/E_{470}$  is known to correlate with the degree of condensation of DOM aromatic  
528 groups and with the degree of humification (Chin et al., 1994; Hur et al., 2006) whereas  $\text{UV}_{254}$

529 is used as proxy for aromatic C and source of DOM (Chen et al., 1977; Uyguner and Bekbolet,  
530 2005). The optical properties of DOC were much less conservative under sunlight exposure  
531 compared to total dissolved C concentration, as  $UV_{254\text{ nm}}$  and  $E_{365}/E_{470}$  ratio sizably decreased in  
532 the course of experiments. Numerous studies of allochthonous riverine DOM also revealed that  
533 photodegradation of colored DOM (CDOM) and  $SUVA_{254}$  were much greater than DOC losses  
534 (Spencer et al., 2009; Reche et al., 2000; Vähätalo and Wetzel, 2004; Mostofa et al., 2011; Bittar  
535 et al., 2015; Gareis and Lesack, 2018). A decrease of  $E_{365}/E_{470}$  corresponded to removal of UV  
536 rather than visual light absorbing functional groups, whereas a constant pattern of  $E_{254}/E_{436}$  ratio  
537 within the hydrological continuum 'depression → stream → lake → river' was consistent with  
538 lack of autochthonous DOM in all studied water objects, which were dominated by terrestrial  
539 (aromatic) DOM from peat horizons. Overall, our observations confirm the conclusion achieved  
540 from a recent compilation of available data across the world that degradation processes act  
541 preferentially on CDOM rather than DOC concentration (Massicotte et al., 2017; Oleinikova et  
542 al., 2017).

543 In contrast to DOC, sizeable removal of dissolved P and Fe together with some related  
544 trace elements (Ti, V, Zn, Nb) during photolysis of surface waters reflects transformation and  
545 coagulation of Fe-rich colloids, that behave independent on organic colloids in humic waters  
546 (Vasyukova et al., 2010; Pokrovsky et al., 2016). This precipitation of Fe hydroxides together  
547 with P and insoluble trace elements was mostly pronounced in permafrost stream which had the  
548 highest pH. In this stream, Fe(III) hydroxide was not stable due to pronounced hydrolysis. After  
549 photolytic removal of small amount of DOM that stabilized colloidal Fe (Oleinikova et al., 2017),  
550 Fe hydroxide could coagulate and coprecipitate P and some trace elements.

551

552

553           4.3. *Lack of bio- and photodegradation in humic surface waters of frozen peat bogs*  
554 *despite sizeable CO<sub>2</sub> emission*

555           The main result of the present study is that, despite well-known supersaturation of lentic  
556 and lotic waters of frozen peatlands to atmospheric pCO<sub>2</sub> (Serikova et al., 2018, 2019), these  
557 waters exhibit negligible bio- and photo-degradability over time scale (28 days) comparable with  
558 or exceeding the water residence time in various reservoirs. For consistency with other studies in  
559 high latitudes, we assessed the bio- and photodegradability of DOM during middle summer  
560 period. Non-accounting for the spring freshet, which represents more than 60% of annual DOM  
561 transport in similar boreal and subarctic rivers of European Russia (Pokrovsky et al., 2010) and  
562 western Siberia (Pokrovsky et al., 2015; Vorobyev et al., 2019), may create substantial bias when  
563 extending our results to other territories of the subarctic during full open water period. However,  
564 it was recently shown that during spring flood, the DOM in the largest European Arctic River,  
565 Severnaya Dvina, which is similar to the Pechora River, is not at all biodegradable (Shirokova et  
566 al., 2017b). Moreover, the spring-time period does not exhibit any particularly high C  
567 concentrations in thaw ponds and thermokarst lake waters of frozen peatlands (Manasypov et al.,  
568 2015), and CO<sub>2</sub> emissions from rivers and lakes of permafrost-affected wetlands of western  
569 Siberia were not much higher in spring compared to other seasons (Serikova et al., 2018, 2019).  
570 Therefore, although our seasonally-restricted data set is not representative for the pan Arctic  
571 environment and further studies with high spatial resolution across different climate zones are  
572 needed (see examples in Lapierre and del Giorgio, 2014), our findings are at odds with the  
573 dominant paradigm that bio- and photodegradation control the DOC removal from arctic aquatic  
574 ecosystems (Abbot et al., 2014; Cory et al., 2014; Spencer et al., 2015). Given incontestable bio-  
575 and photodegradability of peat pore waters and frozen soil extracts reported across the Arctic  
576 (Vonk et al., 2015; Selvam et al., 2017), this strongly suggests that the DOM that arrives to small  
577 rivers and even permafrost depressions via lateral peat soil outflux is already highly degraded.

578 This is consistent with general idea that rates of DOM photochemical alteration and rates of  
579 microbial responses to altered DOM are typically rapid, from minutes to days (Cory and Kling,  
580 2018). As such, the majority of elevated CO<sub>2</sub> measured in surface waters of permafrost peat  
581 landscape originates from degradation of soil water DOM once it enters open surface water. This  
582 is especially true for photo-oxidation, which is not likely to occur in the soil.

583 We believe that the degradation of soil DOM in surface waters of frozen peatlands occurs  
584 very fast and completes within first hours or days. This is shorter than the residence time of water  
585 in permafrost depressions, thaw ponds and rivers (Manasypov et al., 2015). As a result, we did  
586 not detect sizeable bio- and photodegradation of residual DOM in various types of inland waters  
587 from permafrost landscapes. In order to explain persistent CO<sub>2</sub> supersaturation of inland waters  
588 from peatlands, we suggest that benthic respiration of stream, lake and river sediments produce  
589 sizeable amount of CO<sub>2</sub> thus increasing overall C emission potential of the aquatic systems  
590 (MacIntyre et al., 2018; Valle et al., 2018). For example, anaerobic C mineralization of  
591 thermokarst lake sediments is fairly well established in discontinuous permafrost zone of peat  
592 bogs in western Siberia (Audry et al., 2011) and Canada (Deshpande et al., 2017). Note that the  
593 potential for dark DOM chemical oxidation in iron-rich organic-rich waters facing redox  
594 oscillation (i.e., Page et al., 2012) is rather low in studied thermokarst waters which remain  
595 essentially oxic over full depth of the water column during unfrozen period of the year.

596 The findings of this study and widely reported dominance of non-biodegradable DOC (0-  
597 1% BDOC) in large rivers and streams of the non-permafrost zone (Vonk et al., 2015) suggest  
598 that 1) the majority of BDOC is degraded before its arrival to large aquatic reservoirs, and 2) the  
599 CO<sub>2</sub> supersaturation and emission of surface waters from frozen peatlands is due to soil pore  
600 water and sediment respiration rather than aerobic bio- and photo-degradation of DOM in the  
601 water column. Further, the non-increase in BDOC fraction during temperature rise from 4 to  
602 37°C implies that, within the climate warming scenario, the heating of peat surface waters will



603 be a minor factor of overall CO<sub>2</sub> balance. Instead, the change of water path and residence time in  
604 pore waters of frozen peatlands, the rate of supra-permafrost water delivery, and the magnitude  
605 of benthic respiration in large rivers and thermokarst lakes may control the CO<sub>2</sub> emission from  
606 inland waters.

607

## 608 **Conclusions**

609 This work revealed high resistance of surface waters collected in permafrost peatland to  
610 both bio- and photo-degradation. Less than 5-10% of the initial aquatic DOC was removed over  
611 1 month of dark aerobic incubation at 4, 22 and 37°C as well as during sunlight exposure of  
612 sterile-filtered waters. In contrast to expected differences in bio- and photo-lability between small  
613 permafrost subsidences, streams, large lake and the Pechora River, there was no measurable  
614 difference in surface waters BDOC concentration along the hydrological continuum. The  
615 contribution of aerobic DOM biodegradation within the water column to observed CO<sub>2</sub>  
616 supersaturations and net CO<sub>2</sub> emission fluxes from bog water, lakes, streams and rivers of  
617 peatland territories located within discontinuous permafrost zone is less than 10%. Despite  
618 decrease in CDOM during photolysis, this process does not significantly contribute to total DOC  
619 degradation and C emission from the surface of inland waters of frozen peatlands.

620 We hypothesize that refractory nature of DOM from frozen peatlands which is already  
621 processed in soil waters before arriving to lentic and lotic surface reservoirs create unfavorable  
622 conditions for biodegradation. The reason for high stability of DOM from frozen peatland to  
623 photolysis is less clear but can be linked to fast photo-degradation of peat bog and soil shallow  
624 underground) waters after their exposure to the surface, occurring within the first hours to days.  
625 We conclude on negligible impact of **separate** bio- and photo-degradation on DOM processing **ing**  
626 **and CO<sub>2</sub> emission in surface waters of frozen peatlands.** This calls for future work to quantify

627 the combined bio- and photo-lability of peat pore waters, thawing soil ice, and suprapermafrost  
628 flow, which deliver the DOM to the rivers, lakes and depressions.

629

### 630 **Acknowledgements**

631 This work was supported by RFFI (RFBR) grants No 17-05-00348\_a and 17-05-00342\_a,  
632 Program FANO No 0409-2015-0140, RFFI No 18-05-01041 and UroRAN No 18-9-5-29.  
633 Additional funding from JPI Climate initiative, financially supported by VR (the Swedish  
634 Research Council) grant no. 325-2014-6898, is also acknowledged.

635

### 636 **References**

- 637 Abbott, B. W., Larouche, J. R., Jones, J. B., Bowden, W. B., and Balsler, A. W.: Elevated  
638 dissolved organic carbon biodegradability from thawing and collapsing permafrost, *J.*  
639 *Geophys. Res.*, 119, 2049–2063, 2014.
- 640 Amado, A. M., Cotner, J. B., Cory, R. M., Edhlund, B. L., and McNeill, K.: Disentangling the  
641 interactions between photochemical and bacterial degradation of dissolved organic matter:  
642 amino acids play a central role, *Microb. Ecol.*, 69(3), 554-566, 2014.
- 643 Andersson, M. G. I., Catalán, N., Rahman, Z., Tranvik, L. J., and Lindström, E. S.: Effects of  
644 sterilization on dissolved organic carbon (DOC) composition and bacterial utilization of  
645 DOC from lakes, *Aquat. Microb. Ecol.*, 82, 199-208, 2018.
- 646 Ask, J., Karlsson, J., and Jansson, M.: Net ecosystem production in clear-water and brown-water  
647 lakes, *Glob. Biogeochem. Cycles*, 26, GB1017, doi:10.1029/2010GB003951, 2012.
- 648 Audry, S., Pokrovsky, O. S., Shirokova, L. S., Kirpotin, S. N., and Dupré, B.: Organic matter  
649 mineralization and trace element post-depositional redistribution in Western Siberia  
650 thermokarst lake sediments, *Biogeosciences*, 8, 3341-3358, 2011.
- 651 Berggren, M., Laudon, H., Haei, M., Ström, L., and Jansson, M.: Efficient aquatic bacterial  
652 metabolism of dissolved low-molecular-weight compounds from terrestrial sources, *ISME*  
653 *J.*, 4, 408-416, 2010.
- 654 Bittar, T. B., Vieira, A. A. H., Stubbins, A., and Mopper, K.: Competition between  
655 photochemical and biological degradation of dissolved organic matter from the  
656 cyanobacteria *Microcystis aeruginosa*, *Limnol. Oceanogr.*, 60, 1172-1194, 2015.
- 657 Brittain, J. F., Gislason, G. M., Ponomarev, V. I., Bogen, J., Jensen, A. J., Khokhlova, L. G.,  
658 Kochanov, S. K., Kokovkin, A. V., Melvold, K., Olafsson, J. S., Pettersson, L.-E., and  
659 Stenina, A. S.: Arctic Rivers (chapter 9), pp. 337-379. In: *Rivers of Europe*, Eds: Tockner  
660 K., Uehlinger U., Robinson C.T., Academic Press Elsevier, 2009.
- 661 Chen, Y., Senesi, N., and Schnitzer, M.: Information provided on humic substances by E4/E6  
662 ratios, *Soil Sci. Soc. Amer. J.*, 41, 352-358, 1977.
- 663 Chin, Y.-P., Aiken, G., and O'Loughlin, E.: Molecular weight, polydispersity, and spectroscopic  
664 properties of aquatic humic substances. *Environ. Sci. Technol.*, 28, 1853-1858, 1994.
- 665 Chupakova, A. A., Chupakov, A. V., Neverova, N. V., Shirokova, L. S., and Pokrovsky, O. S.:  
666 Photodegradation of river dissolved organic matter and trace metals in the largest European  
667 Arctic estuary. *Sci. Total Environ.*, 622–623, 1343–1352, 2018.

668 Cole, J. J. and Caraco, N. : Atmospheric exchange of carbon dioxide in a low-wind oligotrophic  
669 lake measured by the addition of SF<sub>6</sub>. *Limnol. Oceanogr.*, 43, 647–656, 1998.

670 Cory, R. M., McKnight, D., Chin, Y. P., Miller, P., and Jaros, C. L.: Chemical characteristics of  
671 fulvic acids from Arctic surface waters: Microbial contributions and photochemical  
672 transformations, *J. Geophys. Res.*, 112, G04S51, doi:10.1029/2006JG000343, 2007.

673 Cory, R. M., Crump, B. C., Dobkowski, J. A., and Kling, G. W.: Surface exposure to sunlight  
674 stimulates CO<sub>2</sub> release from permafrost soil carbon in the Arctic, *Proc. Natl. Acad. Sci. USA*,  
675 110(9), 3429-3434, 2013.

676 Cory, R. M., Ward, C. P., Crump, B. C., and Kling, G. W.: Sunlight controls water column  
677 processing of carbon in arctic fresh waters, *Science*, 345, 925-928, 2014.

678 Cory, R. M., Harrold, K. H., Neilson, B. T., Kling, G. W.: Controls on dissolved organic matter  
679 (DOM) degradation in a headwater stream: the influence of photochemical and hydrological  
680 conditions in determining light-limitation or substrate-limitation of photo-degradation,  
681 *Biogeosciences*, 12, 6669–6685, 2015.

682 Cory, R. M., Kling, G. W.: Interactions between sunlight and microorganisms influence  
683 dissolved organic matter degradation along the aquatic continuum, *Limnol. Oceanogr. Lett.*,  
684 3, 102–116, 2018.

685 Dean, J. F., van Hal, J. R., Dolman, A. J., Aerts, R., and Weedon, J. T.: Filtration artefacts in  
686 bacterial community composition can affect the outcome of dissolved organic matter  
687 biolability assays, *Biogeosciences*, 15, 7141-7154, [https://doi.org/10.5194/bg-15-7141-](https://doi.org/10.5194/bg-15-7141-2018)  
688 2018, 2018.

689 Dean, J. F., Garnett, M. H., Spyrakos, E., Billett, M. F.: The potential hidden age of dissolved  
690 organic carbon exported by peatland streams, *J. Geophys. Res.: Biogeosciences*,  
691 124, 328–341, 2019.

692 Deshpande, B. N., Maps, F., Matveev, A., and Vincent, W. F., 2017. Oxygen depletion in  
693 subarctic peatland thaw lakes, *Arctic Science*, 3(2), 406-428, 2017.

694 Deshpande, B. N., Crevecoeur, S., Matveev, A., and Vincent, W. F.: Bacterial production in  
695 subarctic peatland lakes enriched by thawing permafrost, *Biogeosciences*, 13, 4411-4427,  
696 2016.

697 Drake, T. W., Holmes, R. M., Zhulidov, A. V., Gurtovaya, T., Raymond, P. A., McClelland, J.  
698 W., and Spencer, R. G. M.: Multidecadal climate-induced changes in Arctic tundra lake  
699 geochemistry and geomorphology, *Limnol. Oceanogr.*, 64, S179-S191, 2019.

700 Gao, L., Zhou, Z., Reyes, A. V., and Guo, L.: Yields and characterization of dissolved organic  
701 matter from different aged soils in northern Alaska, *J. Geophys. Res.: Biogeosciences*, 123,  
702 2035–2052, 2018.

703 Gareis, J. A. L., and Lesack, L. F. W.: Photodegraded dissolved organic matter from peak freshet  
704 river discharge as a substrate for bacterial production in a lake-rich great Arctic delta, *Arctic*  
705 *Science*, 4(4), 557-583, 2018.

706 Groeneveld, M., Tranvik, L., Natchimuthu, S., and Koehler, B.: Photochemical mineralisation in  
707 a boreal brown water lake: considerable temporal variability and minor contribution to  
708 carbon dioxide production, *Biogeoscience*, 13, 3931-3943, 2016.

709 Helms, J. R., Stubbins, A., Ritchie, J. D., Minor, E. C., Kieber, D. J., Mopper, K.: Absorption  
710 spectral slopes and slope ratios as indicators of molecular weight, source, and  
711 photobleaching of chromophoric dissolved organic matter, *Limnol. Oceanogr.*, 53(3), 955-  
712 969, 2008.

713 Holmes, R. M., McClelland, J. W., Raymond, P. A., Frazer, B. B., Peterson, B. J., and Stieglitz, M.:  
714 Labiality of DOC transported by Alaskan rivers to the Arctic Ocean, *Geophys. Res. Lett.*, 35,  
715 L03402, doi:10.1029/2007GL032837, 2008.

716 Hulatt, C. J., Kaartokallio, H., Asmala, E., Autio, R., Stedmon, C. A., Sonninen, E., Oinonen,  
717 M., and Thomas, D. N.: Bioavailability and radiocarbon age of fluvial dissolved organic  
718 matter (DOM) from a northern peatland-dominated catchment: effect of land-use change,  
719 *Aquat. Sci.*, 76(3), 393-404, 2014.

720 Hur, J., Williams, M. A., and Schlautman, M. A.: Evaluating spectroscopic and chromatographic  
721 techniques to resolve dissolved organic matter via end member mixing analysis, *Chemosphere*,  
722 63, 387-402, 2006.

723 Ilina, S. M., Drozdova, O. Yu., Lapitsky, S. A., Alekhin, Yu. V., Demin, V. V., Zavgorodnaya, Yu.  
724 A., Shirokova, L. S., Viers, J., and Pokrovsky, O. S.: Size fractionation and optical properties  
725 of dissolved organic matter in the continuum soil solution-bog-river and terminal lake of a  
726 boreal watershed, *Org. Geochem.*, 66, 14–24, 2014.

727 Kaiser, K., Canedo-Oropeza, M., McMahon, R., and Amon, R. M. W.: Origins and  
728 transformations of dissolved organic matter in large Arctic rivers, *Sci. Reports*, 7, 13064,  
729 2017.

730 Karlsson, J., Jansson, M., and Jonsson, A.: Respiration of allochthonous organic carbon in  
731 unproductive forest lakes determined by the Keeling plot method, *Limnol. Oceanogr.*, 52,  
732 603-608, 2007.

733 Koehler, B., Landelius, T., Weyhenmeyer, G. A., Machida, N., and Tranvik, L.J.: Sunlight-  
734 induced carbon dioxide emissions from inland waters, *Global Biogeochem. Cycles*, 28, 696–  
735 711, 2014.

736 Köhler, S., Buffam, I., Jonsson, A., and Bishop, K.: Photochemical and microbial processing of  
737 stream and soil water dissolved organic matter in a boreal forested catchment in northern  
738 Sweden, *Aquat. Sci.*, 64, 269–281, 2002.

739 Lapierre, J.-F., Guillemette, F., Berggren, M., and del Giorgio, P. A.: Increases in terrestrially  
740 derived carbon stimulate organic carbon processing and CO<sub>2</sub> emissions in boreal aquatic  
741 ecosystems, *Nature Comm.*, 4, 2972, doi:10.1038/ncomms3972, 2013.

742 Lapierre, J.-F. and del Giorgio, P. A.: Partial coupling and differential regulation of biologically  
743 and photochemically labile dissolved organic carbon across boreal aquatic networks,  
744 *Biogeosciences*, 11, 5969-5985, <https://doi.org/10.5194/bg-11-5969-2014>, 2014.

745 Larouche, J. R., Abbott, B. W., Bowden, W. B., Jones, and J. B.: The role of watershed  
746 characteristics, permafrost thaw, and wildfire on dissolved organic carbon biodegradability  
747 and water chemistry in Arctic headwater streams, *Biogeosciences*, 12, 4221-4233, 2015.

748 Laurion, I., and Mladenov, N.: Dissolved organic matter photolysis in Canadian Arctic thaw  
749 ponds, *Environ. Res. Lett.*, 8, 035026, doi.org/10.1088/1748-9326/8/3/035026, 2013.

750 Logue, J. B., Stedmon, C. A., Kellerman, A. M., Nielsen, N. J., Andersson, A. F., Laudon, H.,  
751 Lindström, E. S., and Kritzberg, E. S.: Experimental insights into the importance of aquatic  
752 bacterial community composition to the degradation of dissolved organic matter, *ISME J.*,  
753 10, 533–545, 2016.

754 Lou, T., and Xie, H.: Photochemical alteration of the molecular weight of dissolved organic  
755 matter, *Chemosphere*, 65, 2333-2342, 2006.

756 MacIntyre, S., Cortes, A., and Sadro, S.: Sediment respiration drives circulation and production  
757 of CO<sub>2</sub> in ice-covered Alaskan arctic lakes, *Limnol. Oceanogr. Lett.*, 3, 302–310, 2018.

758 Manasypov, R. M., Pokrovsky, O. S., Kirpotin, S. N., Shirokova, L. S.: Thermokarst lake waters  
759 across permafrost zones of Western Siberia, *Cryosphere* 8, 1177-1193, 2014.

760 Manasypov, R. M., Vorobyev, S. N., Loiko, S. V., Kritzkov, I. V., Shirokova, L. S., Shevchenko,  
761 V. P., Kirpotin, S. N., Kulizhsky, S. P., Kolesnichenko, L. G., Zemtsov, V. A., Sinkinov, V.  
762 V., and Pokrovsky, O. S.: Seasonal dynamics of organic carbon and metals in thermokarst  
763 lakes from the discontinuous permafrost zone of western Siberia, *Biogeosciences*, 12, 3009-  
764 3028, 2015.

765 Mann, P. J., Davydova, A., Zimov, N., Spencer, R. G. M., Davydov, S., Bulygina, E., Zimov, S.,  
766 Holmes, R. M.: Controls on the composition and lability of dissolved organic matter in  
767 Siberia's Kolyma River basin, *J. Geophys. Res.*, 117, G01028, doi: 10.1029/2011JG001798,  
768 2012.

769 Mann, P. J., Sobczak, W. V., LaRue, M. M., Bulygina, E., Davydova, A., Vonk, J. E., Schade,  
770 J., Davydov, S., Zimov, N., Holmes, R. M., Spencer, R. G. M.: Evidence for key enzymatic  
771 controls on metabolism of Arctic river organic matter, *Global Change Biol.*, 20(4), 1089-  
772 1100, 2014.

773 Mann, P. J., Eglinton, T. I., McIntyre, C. P., Zimov, N., Davydova, A., Vonk, J. E., Holmes, R.  
774 M., Spencer, R. G. M.: Utilization of ancient permafrost carbon in headwaters of Arctic  
775 fluvial networks, *Nat. Commun.*, 6, doi: 10.1038/ncomms8856, 2015.

776 Massicotte, P., Asmala, E., Stedmon, C., Markager, S.: Global distribution of dissolved matter  
777 along the aquatic continuum: Across rivers, lakes and oceans, *Sci. Total Environ.*, 609, 180-  
778 191, 2017.

779 McCallister, S. L., and del Giorgio, P. A.: Direct measurement of the  $\delta^{13}\text{C}$  signature of carbon  
780 respired by bacteria in lakes: Linkages to potential carbon sources, ecosystem baseline  
781 metabolism, and  $\text{CO}_2$  fluxes, *Limnol. Oceanogr.*, 53(4), 1204–1216, 2008.

782 Moody, C. S., Worrall, F., Evans, C. D., Jones, T. G.: The rate of loss of dissolved organic carbon  
783 (DOC) through a catchment, *J. Hydrol.*, 492, 139-150, 2013.

784 Moran, M. A., Sheldon, W. M., and Zepp, R. G.: Carbon loss and optical property changes during  
785 long-term photochemical and biological degradation of estuarine dissolved organic matter,  
786 *Limnol. Oceanogr.*, 45, 1254–1264, 2000.

787 Mostofa, K. M. G., Yoshioka, T., Konohira, E., and Tanoue, E.: Photodegradation of fluorescent  
788 dissolved organic matter in river waters, *Geochem. J.*, 41, 323-331, 2007.

789 Mostofa, K. M. G., Wu, F., Liu, C-Q., Vione, D., Yoshioka, T., Sakugawa, H., and Tanoue, E.:  
790 Photochemical, microbial and metal complexation behavior of fluorescent dissolved organic  
791 matter in the aquatic environments, *Geochem. J.*, 45, 235-254, 2011.

792 Novikov, S. M., Moskvina, Y. P., Trofimov, S. A., Usova, L. I., Batuev, V. I., Tumanovskaya, S. M.,  
793 Smirnova, V. P., Markov, M. L., Korotkevich, A. E., and Potapova, T. M.: Hydrology of bog  
794 territories of the permafrost zone of western Siberia, *BBM publ. House, St. Petersburg*, 535  
795 pp. (in Russian), 2009.

796 Oleinikova, O., Drozdova, O. Y., Lapitskiy, S. A., Bychkov, A. Y., and Pokrovsky, O. S.:  
797 Dissolved organic matter degradation by sunlight coagulates organo-mineral colloids and  
798 produces low-molecular weight fraction of metals in boreal humic waters, *Geochim.*  
799 *Cosmochim. Acta*, 211, 97-114, 2017.

800 Oleinikova, O., Shirokova, L. S., Drozdova, O. Y., Lapitskiy, S. A., and Pokrovsky, O. S.: Low  
801 biodegradability of dissolved organic matter and trace metal from subarctic waters by culturable  
802 heterotrophic bacteria, *Sci. Total Environ.*, 618, 174-187, 2018.

803 Page, S. E., Sander, M., Arnold, W. A., and McNeill, K.: Hydroxyl radical formation upon  
804 oxidation of reduced humic acids by oxygen in the dark, *Environ. Sci. Technol.*, 46, 1590-  
805 1597, 2012.

806 Peacock, M., Evans, C. D., Fenner, N., Freeman, C., Gough, R., Jones, T. G., and Lebron, I.:  
807 UV-visible absorbance spectroscopy as a proxy for peatland dissolved organic carbon  
808 (DOC) quantity and quality: considerations on wavelength and absorbance degradation,  
809 *Environmental Science: Processes and Impacts*, 10–12, doi:10.1039/c4em00108g, 2014

810 Pickard, A. E., Heal, K. V., McLeod, A. R., and Dinsmore, K. J.: Temporal changes in  
811 photoreactivity of dissolved organic carbon and implications for aquatic carbon fluxes from  
812 peatlands, *Biogeosciences*, 14, 1793-1809, <https://doi.org/10.5194/bg-14-1793-2017>, 2017.

813 Pokrovsky, O. S., Viers, J., Shirokova, L. S., Shevchenko, V. P., Filipov, A. S., and Dupré, B.:  
814 Dissolved, suspended, and colloidal fluxes of organic carbon, major and trace elements in  
815 Severnaya Dvina River and its tributary, *Chem. Geology*, 273, 136–149, 2010.

816 Pokrovsky, O. S., Shirokova, L. S., Zabelina, S. A., Vorobieva, T. Ya., Moreva, O. Yu., Klimov,  
817 S. I., Chupakov, A. V., Shorina, N. V., Kokryatskaya, N. M., Audry, S., Viers, J., Zoutien,  
818 C., and Freyrier, R.: Size fractionation of trace elements in a seasonally stratified boreal  
819 lakes: Control of organic matter and iron colloids, *Aquat. Geochem.*, 18, 115–139, 2012.

820 Pokrovsky, O. S., Shirokova, L. S., Kirpotin, S. N., Kulizhsky, S. P., Vorobiev, S. N.: Impact of  
821 Western Siberia heat wave 2012 on greenhouse gases and trace metal concentration in thaw  
822 lakes of discontinuous permafrost zone, *Biogeosciences*, 10, 5349–5365, 2013.

823 Pokrovsky, O. S., Manasypov, R. M., Shirokova, L. S., Loiko, S. V., Krickov, I. V., Kopysov,  
824 S., and Kirpotin, S. N.: Permafrost coverage, watershed area and season control of dissolved  
825 carbon and major elements in western Siberia rivers, *Biogeosciences*, 12, 6301–6320, 2015.

826 Pokrovsky, O. S., Manasypov, R. M., Loiko, S. V., and Shirokova, L. S.: Organic and organo-  
827 mineral colloids of discontinuous permafrost zone, *Geochim. Cosmochim. Acta*, 188, 1–20,  
828 2016.

829 Porcal, P., Dillon, P. J., and Molot, L. A.: Photochemical production and decomposition of  
830 particulate organic carbon in a freshwater stream, *Aquat. Sci.*, 75, 469–482, 2013.

831 Porcal, P., Dillon, P. J., and Molot, L. A.: Interaction of extrinsic chemical factors affecting  
832 photodegradation of dissolved organic matter in aquatic ecosystems, *Photochem. Photobiol.*  
833 *Sci.*, 13, 799–812, 2014.

834 Porcal, P., Dillon, P. J., and Molot, L. A.: Temperature dependence of photodegradation of  
835 dissolved organic matter to dissolved inorganic carbon and particulate organic carbon, *Plos*  
836 *ONE*, 10(6), e0128884, DOI:10.1371/journal.pone.0128884, 2015.

837 Porter, K. G., and Feig, Y. S.: The use of DAPI for identifying and counting aquatic microflora,  
838 *Limnol. Oceanogr.*, 25: 943–948, 1980.

839 Raudina, T. V., Loiko, S. V., Lim, A., Manasypov, R. M., Shirokova, L. S., Istigecegev, G. I.,  
840 Kuzmina, D. M., Kulizhsky, S. P., Vorobyev, S. N., and Pokrovsky, O. S.: Permafrost thaw  
841 and climate warming may decrease the CO<sub>2</sub>, carbon, and metal concentration in peat soil  
842 waters of the Western Siberia Lowland, *Sci. Total Environ.*, 634, 1004–1023, 2018.

843 Reader, H. E., Stedmon, C. A., and Kritzberg, E. S.: Seasonal contribution of terrestrial organic  
844 matter and biological oxygen demand to the Baltic Sea from three contrasting river  
845 catchments, *Biogeosciences* 11, 3409–3419, 2014.

846 Reche, I., Pace, M. L., and Cole, J. J.: Modeled effects of dissolved organic carbon and solar  
847 spectra on photobleaching in lake ecosystems, *Ecosystems* 3, 419–432, 2000.

848 Roehm, C. L., Giesler, R., Karlsson, J.: Bioavailability of terrestrial organic carbon to lake  
849 bacteria: The case of a degrading subarctic permafrost mire complex, *J. Geophys. Res.*, 114,  
850 G03006, doi: 10.1029/2008JG000863, 2009.

851 Selvam, B. P., Lapierre, J.-F., Guillemette, F., Voigt, C., Lamprecht, R. E., Biasi, C., Christensen,  
852 T. R., Martikainen P. J., and Berggren, M.: Degradation potentials of dissolved organic  
853 carbon (DOC) from thawed permafrost peat. *Scientific Reports*, 7, Art No 45811, doi:  
854 10.1038/srep45811, 2016.

855 Serikova, S., Pokrovsky, O. S., Ala-aho, P., Kazantsev, V., Kirpotin, S. N. Kopysov, S. G.,  
856 Krickov, I. V., Laudon, H., Manasypov, R. M., Shirokova, L. S., Sousby, C., Tetzlaff, D.,  
857 Karlsson, J.: High riverine CO<sub>2</sub> emissions at the permafrost boundary of Western Siberia.  
858 *Nature Geoscience*, 11, 825–829, 2018.

859 Serikova S., Pokrovsky O. S., Laudon, H., Krickov, I. V., Lim, A. G., Manasypov, R. M.,  
860 Karlsson, J.: C emissions from lakes across permafrost gradient of Western Siberia. *Nature*  
861 *Comm.*, 10, Art No 1552, <https://doi.org/10.1038/s41467-019-09592-1>, 2019.

862 Shirokova, L. S., Pokrovsky, O. S., Moreva, O. Y., Chupakov, A. V., Zabelina, S. A., Klimov,  
863 S. I., Shorina, N. V., and Vorobieva T. Y.: Decrease of concentration and colloidal fraction  
864 of organic carbon and trace elements in response to the anomalously hot summer 2010 in a  
865 humic boreal lake, *Sci. Tot. Environ.*, 463-464, 78–90, 2013a.

866 Shirokova, L. S., Pokrovsky, O. S., Kirpotin, S. N., Desmukh, C., Pokrovsky, B. G., Audry, S.,  
867 and Viers, J.: Biogeochemistry of organic carbon, CO<sub>2</sub>, CH<sub>4</sub>, and trace elements in  
868 thermokarst water bodies in discontinuous permafrost zones of Western Siberia,  
869 *Biogeochemistry*, 113, 573–593, 2013b.

870 Shirokova, L. S., Bredoire, R., Rolls, J. L., and Pokrovsky, O. S.: Moss and peat leachate  
871 degradability by heterotrophic bacteria: fate of organic carbon and trace metals,  
872 *Geomicrobiol. J.*, 34(8), 641-655, 2017a.

873 Shirokova, L. S., Chupakova, A. A., Chupakov, A. V., and Pokrovsky, O.S.: Transformation of  
874 dissolved organic matter and related trace elements in the mouth zone of the largest European  
875 Arctic river: experimental modeling, *Inland Waters*, 7(3), 272-282, 2017b.

876 Spencer, R. G. M., Stubbins, A., Hernes, P. J., Baker, A., Mopper, K., Aufdenkampe, A. K.,  
877 Dyda, R. Y., Mwamba, V. L., Mangangu, A. M., Wabakanghanzi, J. N., and Six, J.:  
878 Photochemical degradation of dissolved organic matter and dissolved lignin phenols from  
879 the Congo River, *J. Geophys. Res.*, 114, G03010, doi: 10.1029/2009JG000968, 2009.

880 Spencer, R. G. M., Mann, P. J., Dittmar, T., Eglinton, T. I., McIntyre, C., Holmes, R. M., Zimov,  
881 N., Stubbins, A.: Detecting the signature of permafrost thaw in Arctic rivers, *Geophys. Res.*  
882 *Lett.*, 42, 2830-2835, 2015.

883 Stubbins, A., Mann, P. J., Powers, L., Bittar, T. B., Dittmar, T., McIntyre, C. P., Eglinton, T. I.,  
884 Zimov, N., and Spencer, R. G. M.: Low photolability of yedoma permafrost dissolved  
885 organic carbon, *J. Geophys. Res. Biogeosci.*, 122, 200-211, doi: 10.1002/2016JG003688,  
886 2017.

887 Stutter, M. I., Richards, S., and Dawson, J. J. C.: Biodegradability of natural dissolved organic  
888 matter collected from a UK moorland stream, *Water Res.*, 47(3), 1169-1180, 2013.

889 Sulzberger, B., Austin, A. T., Cory, R. M., Zepp, R. G., and Paul, N. D.: Solar UV radiation in  
890 a changing world: roles of cryosphere-land-water-atmosphere interfaces in global  
891 biogeochemical cycles, *Photochem. Photobiol. Sci.*, doi: 10.1039/c8pp90063a, 2019.

892 Tarnocai, C., Canadell, J. G., E. Schuur A. G., Kuhry P., Mazhitova G., and Zimov S.: Soil  
893 organic carbon pools in the northern circumpolar permafrost region, *Global Biogeochem.*  
894 *Cy.*, 23, GB2023, <https://doi.org/10.1029/2008GB003327>, 2009.

895 Textor, S. R., Guillemette, F., Zito, P. A., Spencer, R. G. M.: An assessment of dissolved  
896 organic carbon biodegradability and priming in blackwater systems, *J. Geophys. Res.*  
897 *Biogeosciences*, 123(9), 2998-3015, 2018.

898 Uyguner, C., and Bekbolet, M. : Implementation of spectroscopic parameters for practical  
899 monitoring of natural organic matter, *Desalination*, 176, 47-55, 2005.

900 Valle, J., Gonsior, M., Hairir, M., Enrich-Prast, A., Schmitt-Kopplin, P., Bastviken, D., Conrad  
901 R., and Hertkorn, N.: Extensive processing of sediment pore water dissolved organic  
902 matter during anoxic incubation as observed by high-field mass spectrometry (FTICR-  
903 MS), *Water Research*, 129, 252-263, 2018.

904 Vähätalo, A. V., Salonen, K., Münster, U., Järvinen, M., and Wetzel, R. G.: Photochemical  
905 transformation of allochthonous organic matter provides bioavailable nutrients in a humic  
906 lake, *Acta Hydrobiol.*, 156, 287-314, 2003.

907 Vähätalo, A. V. and Wetzel, R.G.: Photochemical and microbial decomposition of chromophoric  
908 dissolved organic matter during long (months-years) exposures, *Mar. Chem.*, 89, 313-326,  
909 2004.

910 Vasyukova, E., Pokrovsky, O. S., Viers, J., Oliva, P., Dupré, B., Martin, F., and Candaudap, F.:  
911 Trace elements in organic- and iron-rich surficial fluids of boreal zone: Assessing colloidal  
912 forms via dialysis and ultrafiltration, *Geochim. Cosmochim. Acta*, 74, 449-468, 2010.

913 Vonk, J. E., Tank, S. E., Mann, P. J., Spencer, R. G. M., Treat, C. C., Striegl, R. G., Abbott,  
914 B. W., and Wickland K. P.: Biodegradability of dissolved organic carbon in permafrost  
915 soils and aquatic systems: a meta-analysis, *Biogeosciences*, 12, 6915-6930, 2015.

916 Vorobyev, S. N., Pokrovsky O. S., Kolesnichenko, L. G., Manasypov, R. M., Shirokova, L. S.,  
917 Karlsson, J., and Kirpotin, S. N.: Biogeochemistry of dissolved carbon, major and trace  
918 elements during spring flood periods on the Ob River, *Hydrol. Processes*, 33(11), 1579-1594,  
919 2019.

920 Ward, C. P., Cory, R. M.: Complete and partial photo-oxidation of dissolved organic matter  
921 draining permafrost soils, *Environ. Sci. Technol.*, 50(7), 3545-3553, 2016.

922 Ward, C. P., Nalven, S. G., Crump, B. C., Kling, G. W., and Cory, R. M.: Photochemical  
923 alteration of organic carbon draining permafrost soils shifts microbial metabolic pathways  
924 and stimulates respiration, *Nature Comm.*, 8, Art No 772, 2017.

925 Wauthy M., Rautio, M., Christoffersen, K. S., Forsstrom, L., Laurion, I., Mariash, H. L., Peura,  
926 S., Vincent, W. F.: Increasing dominance of terrigenous organic matter in circumpolar  
927 freshwaters due to permafrost thaw, *Limnol. Oceanogr. Lett.*, 3, 2018, 186–198, 2012.

928 Weishaar, J. L., Aiken, G. R., Bergamaschi, B. A., Fram, M. S., Fujii, R., Mopper, K.:  
929 Evaluation of specific ultraviolet absorbance as an indicator of the chemical composition  
930 and reactivity of dissolved organic carbon, *Environ. Sci. Technol.*, 37, 4702–4708, 2003.

931 Wickland, K. P., Aiken G. R., Butler K., Dornblaser M. M., Spencer R. G. M., and Striegl R.  
932 G.: Biodegradability of dissolved organic carbon in the Yukon River and its tributaries:  
933 seasonality and importance of inorganic nitrogen. *Glob Biogeochem Cycle* 26,  
934 2012gb004342, 2012.

935 Wilkinson, G. M., Pace, M. L., and Cole, J. J. : Terrestrial dominance of organic matter in north  
936 temperate lakes, *Global. Biogeochem. Cycles* 27, 43-51, 2013.

937 Winter, A. R., Fish, T. A. E., Playle, R. C., Smith, D. S., and Curtis, P. J.: Photodegradation of  
938 natural organic matter from diverse freshwater sources, *Aquat. Toxicol.*, 84, 215-222,  
939 2007.

940

941

942

943

944

945

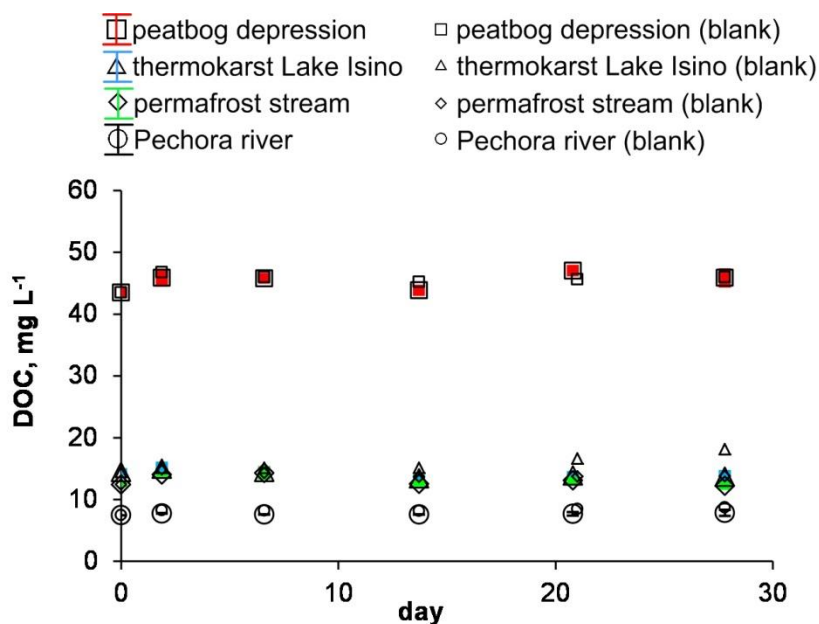
946

947



948

949



950

951

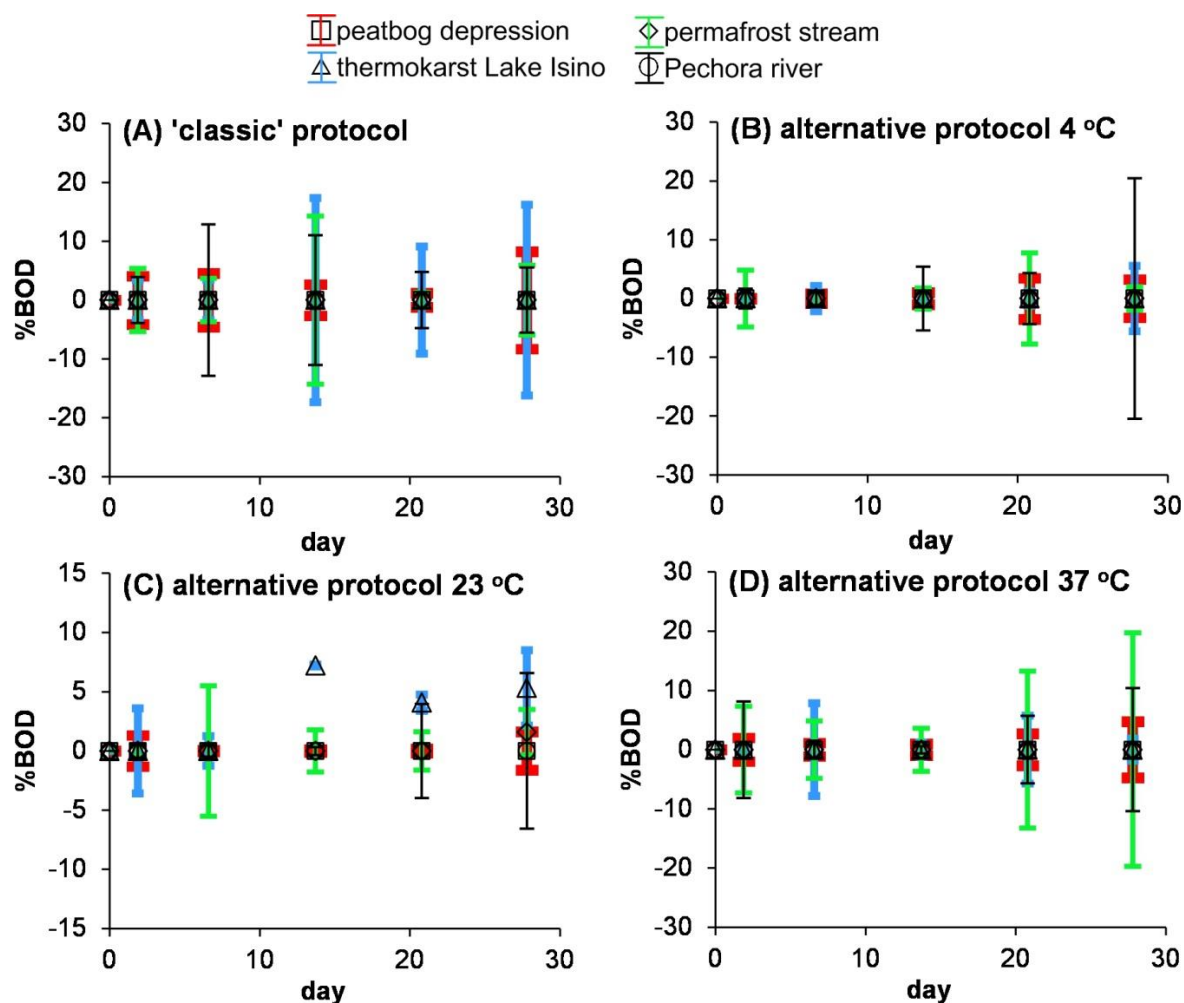
952 **Fig. 1.** The DOC concentration over time in biodegradation experiments at 23°C. The  
953 experiments are shown by solid symbols and the control runs are shown by open symbols: red  
954 squares, peatbog depression; green diamonds, permafrost stream; blue triangles, thermokarst  
955 Lake Isino, and black circles, the Pechora River. The error bars represent 1 s.d. of three replicates  
956 and often within the symbol size.

957

958

959

960



961

962

963

964 **Fig. 2.** Percentage of biodegradable DOC as a function of time. **A**, 'classic' protocol (0.7  $\mu\text{m}$   
 965 GF/F filtration) at 23°C; **B-D**, alternative protocol of 3  $\mu\text{m}$  - filtered solution incubated at 4°C  
 966 (B), 23°C (C) and 37°C (D) and filtered through 0.22  $\mu\text{m}$  at each sampling. The error bars are 1  
 967 s.d. of triplicates or, in a few cases, duplicates.

968

969

970

971

972

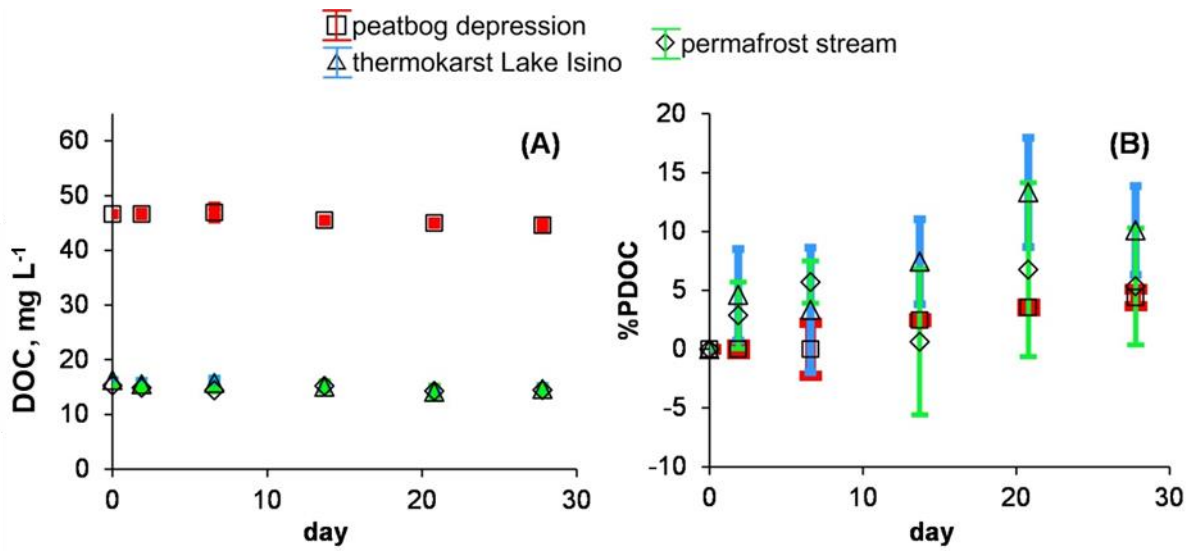
973

974

975

976

977



978

979

980

981 **Fig. 3.** Concentration (A) and percentage of degradable (B) DOC in photo-degradation  
982 experiments. The experiments are shown by solid symbols and the control runs are shown by  
983 open symbols: red squares, peatbog depression; green diamonds, permafrost stream; and  
984 triangles, thermokarst Lake Isino. The error bars are 1 s.d. of triplicates.

985

986

987

988

989

990

991

992

993

994

995

996

997

998

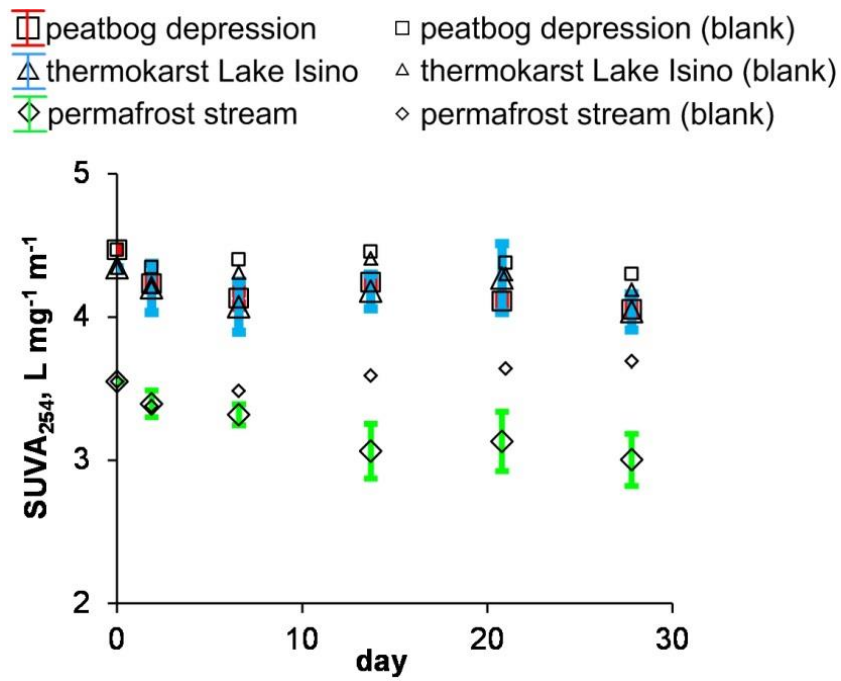
999

1000

1001

1002

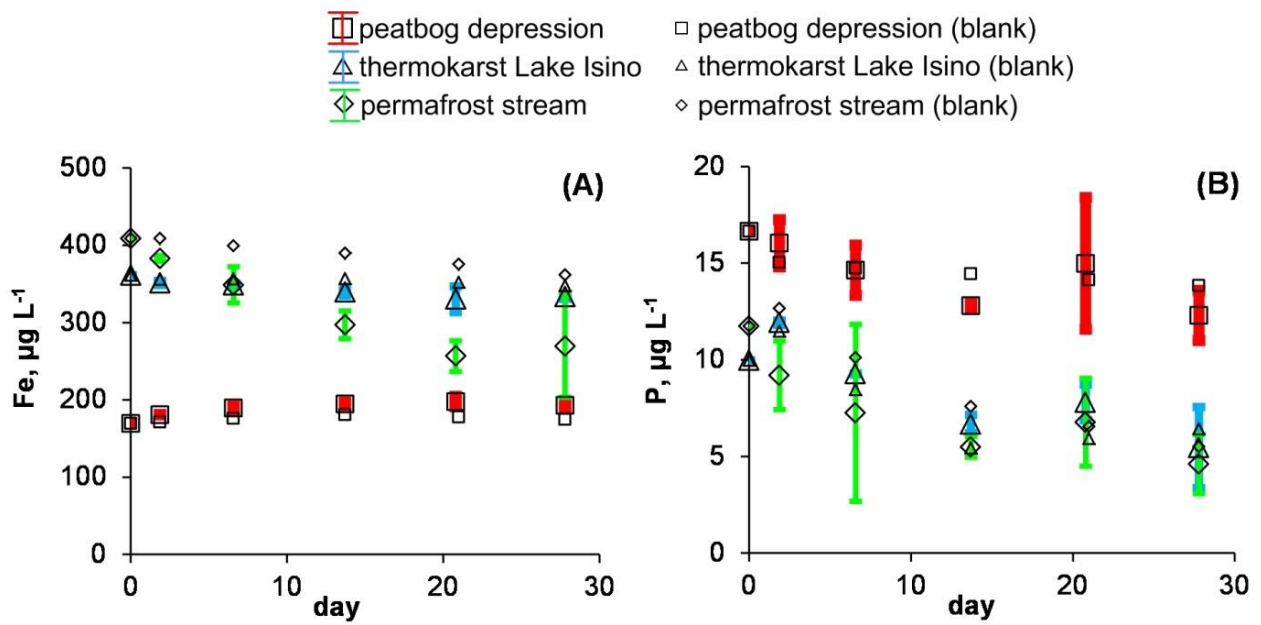
1003  
1004  
1005  
1006  
1007



1008  
1009  
1010  
1011  
1012  
1013  
1014  
1015  
1016  
1017  
1018  
1019  
1020  
1021  
1022  
1023  
1024  
1025  
1026  
1027  
1028

**Fig. 4.**  $SUVA_{254\text{ nm}}$  over time in photo-degradation experiments. The error bars are 1 s.d. of triplicates.

1029  
1030  
1031  
1032



1033  
1034  
1035  
1036  
1037  
1038  
1039  
1040  
1041  
1042  
1043

**Fig. 5.** Fe (A) and P (B) concentration over time in photo-degradation experiments. The error bars are 1 s.d. of triplicates.

1044 **Table 1.** Landscape setting, hydrochemical characteristics and CO<sub>2</sub> concentration and emission flux of studied waters. S.C. is specific  
 1045 conductivity and TBC is total bacteria count (by DAPI).

Sample	BZ-2-17	BZ-24-17	BZ-12	P5
<b>GPS coordinates</b>	67°36'48,8"N, 53°54'29,8"E	67°36.53'N, 53°50.26'E	67°36'47,7"N, 53°54'38,5"E	67°40'09,4", 52°39'30,8"
<b>Description</b>	Depression in peatbog, S <sub>area</sub> = 7.5 m <sup>2</sup>	Stream in frozen peatland, S <sub>watershed</sub> = 7.5 km <sup>2</sup>	Thermokarst lake (Isino), S <sub>area</sub> = 0.005 km <sup>2</sup>	r. Pechora, S <sub>watershed</sub> = 322,000 km <sup>2</sup>
<b>T, °C</b>	24	25	24.1	20
<b>pH</b>	3.85	6.52	5.30	6.92
<b>S.C., μS cm<sup>-1</sup></b>	59.2	31.5	12.9	65.1
<b>DOC, mg L<sup>-1</sup></b>	43.9	16.6	15.6	8.20
<b>DIC, mg L<sup>-1</sup></b>	0.992	2.52	0.808	6.11
<b>SUVA<sub>254</sub></b>	4.08	3.32	4.10	3.82
<b>P-PO<sub>4</sub>, μg L<sup>-1</sup></b>	2.3	9.8	4.4	26.7
<b>P<sub>total</sub>, μg L<sup>-1</sup></b>	14.6	N.D.	7.3	37.5
<b>N-NO<sub>2</sub>, μg L<sup>-1</sup></b>	14.6	5.0	3.6	1.67
<b>N-NO<sub>3</sub>, μg L<sup>-1</sup></b>	14.6	N.D.	76.6	111
<b>N-NH<sub>4</sub>, μg L<sup>-1</sup></b>	13	152	117	36.5
<b>N<sub>total</sub>, μg L<sup>-1</sup></b>	228	N.D.	200	438
<b>Si, μg L<sup>-1</sup></b>	22	392	100	2690
<b>TBC × 10<sup>6</sup>, cell mL<sup>-1</sup></b>	0.81	5.72	5.36	3.51
<b>pCO<sub>2</sub>, ppm</b>	440	2370	1200	1860 (night), 780 (day)
<b>CO<sub>2</sub> flux, mmol m<sup>-2</sup> d<sup>-1</sup></b>	34	30-300*	74	100-130*

1046  
 1047 Footnote: \*, by analogy with small streams of Western Siberian peatlands, of the discontinuous permafrost zone, located in similar  
 1048 environmental context; \*\* By analogy with Taz and Pur Rivers of western Siberian peatlands (Serikova et al., 2018).

1049  
 1050  
 1051